

# How Important Are Functional and Developmental Constraints on Phenotypic Evolution? An Empirical Test with the Stomatal Anatomy of Flowering Plants

Christopher D. Muir,<sup>1,\*</sup> Miquel Àngel Conesa,<sup>2</sup> Jeroni Galmés,<sup>2</sup> Varsha S. Pathare,<sup>3</sup> Patricia Rivera,<sup>4</sup> Rosana López Rodríguez,<sup>5</sup> Teresa Terrazas,<sup>4</sup> and Dongliang Xiong<sup>6</sup>

1. School of Life Sciences, University of Hawaii at Mānoa, Honolulu, Hawaii 96822; 2. Research Group on Plant Biology under Mediterranean Conditions, Departament de Biologia, Universitat de les Illes Balears, Carretera Valldemossa km 7.5, E-07122 Palma, Spain; 3. School of Biological Sciences, Washington State University, Pullman, Washington 99164; 4. Departamento de Botánica, Instituto de Biología, Universidad Nacional Autónoma de México, Apartado Postal 70-367, 04510 Mexico City, Mexico; 5. Departamento de Sistemas y Recursos Naturales, Universidad Politécnica de Madrid, 28040 Madrid, Spain; 6. National Key Laboratory of Crop Genetic Improvement, Ministry of Agriculture (MOA) Key Laboratory of Crop Ecophysiology and Farming System in the Middle Reaches of the Yangtze River, College of Plant Science and Technology, Huazhong Agricultural University, Wuhan, Hubei 430070, China

Submitted October 1, 2021; Accepted October 30, 2022; Electronically published May 1, 2023

Online enhancements: supplemental PDF, Excel table.

**ABSTRACT:** Quantifying the relative contribution of functional and developmental constraints on phenotypic variation is a long-standing goal of macroevolution, but it is often difficult to distinguish different types of constraints. Alternatively, selection can limit phenotypic (co)variation if some trait combinations are generally maladaptive. The anatomy of leaves with stomata on both surfaces (amphistomatous) present a unique opportunity to test the importance of functional and developmental constraints on phenotypic evolution. The key insight is that stomata on each leaf surface encounter the same functional and developmental constraints but potentially different selective pressures because of leaf asymmetry in light capture, gas exchange, and other features. Independent evolution of stomatal traits on each surface imply that functional and developmental constraints alone likely do not explain trait covariance. Packing limits on how many stomata can fit into a finite epidermis and cell size-mediated developmental integration are hypothesized to constrain variation in stomatal anatomy. The simple geometry of the planar leaf surface and knowledge of stomatal development make it possible to derive equations for phenotypic (co)variation caused by these constraints and compare them with data. We analyzed evolutionary covariance between stomatal density and length in amphistomatous leaves from 236 phylogenetically independent contrasts using a robust Bayesian model. Stomatal anatomy on each surface diverges partially independently, meaning that packing limits and developmental integration are not sufficient to explain phenotypic (co)variation. Hence, (co)variation in ecologically important traits like stomata arises in part be-

cause there is a limited range of evolutionary optima. We show how it is possible to evaluate the contribution of different constraints by deriving expected patterns of (co)variance and testing them using similar but separate tissues, organs, or sexes.

**Keywords:** adaptation, amphistomy, developmental integration, leaf, packing limits, phylogenetic comparative methods, stomata.

## Introduction

Selection should move populations toward their multivariate phenotypic optimum if traits can evolve independently and there is sufficient genetic variation. Yet divergence in one trait often covaries with other traits, and covariance can persist for millions of years (Schluter 1996). Covariance is “a rough local measure of the strength of constraint” (Maynard Smith et al. 1985, p. 267) that can be broken down into functional and developmental constraints. Functional constraints are “limitations imposed by time, energy, or the laws of physics” (Arnold 1992, p. S97). In other words, certain trait combinations are not physically or geometrically possible. A classic example is shell coiling among invertebrate lineages in which the morphospace of possible phenotypes is constrained by hard geometrical limits (Raup 1966; McGhee 1999). Within the space of possible phenotypes, developmental constraints can “bias . . . the production of variant phenotypes or [place] a limitation on phenotypic variability” (Maynard Smith et al. 1985, p. 267). For example, Fibonacci leaf arrangement (phyllotaxis)

\* Corresponding author; email: [cdmuir@hawaii.edu](mailto:cdmuir@hawaii.edu).

**ORCID:** Muir, <https://orcid.org/0000-0003-2555-3878>; Galmés, <https://orcid.org/0000-0002-7299-9349>; Pathare, <https://orcid.org/0000-0001-6220-7531>; Xiong, <https://orcid.org/0000-0002-6332-2627>.

may arise from a packing constraint of primordia on the developing apex (Mitchison 1977; Reinhardt and Gola 2022; but for an adaptive explanation, see Niklas 1988). The adaptationist view is that all adaptive areas of trait space are occupied and that natural selection constrains phenotypic variation because maladaptive forms cannot evolve. Under this view, interspecific trait covariation evolves because “missing” maladaptive trait combinations are nonrandomly distributed in trait space. For example, a negative correlation between apparency and toxicity can arise because prey can avoid predation by being cryptic or toxic, but no prey population can exist for long if it is both apparent and palatable. Understanding phenotypic constraint is challenging, but a useful starting point is determining whether phenotypic covariation can be explained by functional or developmental constraints (McGhee 1999, 2007; Olson 2019). If phenotypic covariation is inconsistent with functional and developmental constraints, this provides a strong impetus to test adaptive explanations. This is sometimes referred to as selective constraint because selection eliminates phenotypic variation that is generally maladaptive.

In this study, we will address packing problems and developmental integration, specific forms of functional and developmental constraints relevant to our study system, stomatal anatomy. We introduce these concepts generally in this paragraph. Packing a number of objects into a finite space is a common functional constraint on organisms. Regular geometries that appear in nature, such as helices and hexagons (think DNA and honeycombs), are often optimal solutions to packing problems (Mackenzie 1999; Maritan et al. 2000). Notice that functional constraint does not preclude selection, but the presence of a packing limit changes the range of possible phenotypes. Developmental integration is a form of developmental constraint on multivariate phenotypic evolution, and we use these terms interchangeably in this study. Developmentally integrated traits have a “disposition for covariation” (Armbruster et al. 2014), meaning that evolutionary divergence between lineages in one trait will be tightly associated with divergence in another trait. Allometry is a classic, albeit contested, example of developmental integration that may constrain phenotypic evolution (reviewed in Pélabon et al. 2014). Strong allometric covariation between traits within populations can constrain macroevolutionary divergence for long periods of time depending on the strength and direction of selection (Lande 1979). However, developmental integration does not necessarily hamper adaptation and can even accelerate adaptive evolution when trait covariation is aligned with the direction of selection (Hansen 2003). For example, fusion of floral parts increases their developmental integration, which may increase the rate and precision of multivariate adaptation to specialist polli-

nators (Berg’s rule; Berg 1959, 1960; Armbruster et al. 1999; Conner and Lande 2014).

Stomatal anatomy on the leaves of flowering plants provides an exceptional opportunity to test for functional and developmental constraints because (1) there are thousands of species to compare and (2) the main packing constraints and developmental steps are analytically tractable. This means that it is possible to derive quantitative predictions and test their generality using large comparative data sets representing millions of years of evolutionary history. For this purpose, a heretofore unappreciated fact about stomata is that many leaves have stomata on both lower and upper surfaces. The packing and developmental constraints are the same for stomata on each surface, but the selection may differ. Therefore, if packing and developmental constraints dominate, stomatal anatomy on each surface should diverge in concert. Failure to do so implies that independent evolution is possible and that selection against generally maladaptive phenotypes explains at least some of the covariance between traits. Phylogenetic comparisons of stomatal anatomy provide a statistically powerful, general, and elegant way to distinguish different phenotypic constraints that would be impossible in many other traits with as much ecological significance. The next sections provide background information on stomatal anatomy, how it varies, and why functional or developmental constraints might be important.

#### *How Stomatal Anatomy Varies and Why It Matters*

Stomata are microscopic pores formed by a pair of guard cells that regulate gas exchange ( $\text{CO}_2$  gain and water vapor loss) on the leaves or other photosynthetic surfaces of most land plants. Stomata originated once in the history of land plants around 500 Ma, diversified rapidly in density and size, and have been maintained in most lineages except some bryophytes and aquatic plants (recently reviewed in Clark et al. 2022). Stomata respond physiologically by opening and closing in response to light, humidity, temperature, circadian rhythm, and plant water status (Hetherington and Woodward 2003; Lawson and Matthews 2020). The stomatal size, density, and distribution on a mature leaf do not change, so the maximum rate of gas exchange is fixed. However, the plant may respond plastically to environmental cues, such as light and  $\text{CO}_2$ , by altering stomatal anatomy in new leaves (Casson and Gray 2008). Physiological responses (aperture change) and plastic responses (new leaves with changed anatomy) may be alternative strategies for plants to acclimate to environmental change (Haworth et al. 2013). Finally, stomatal anatomy can evolve because of inherited changes in stomatal development. Plastic and genetic changes in stomatal anatomy are both ecologically important, but most studies do not

use a common garden design that would tease apart their relative contribution.

We focus on anatomical variation in the density, size, and patterning of stomata on a leaf because these factors set the maximum stomatal conductance to CO<sub>2</sub> diffusing into a leaf and the amount of water that transpires from it (Franks and Farquhar 2001; Sack et al. 2003; Galmés et al. 2013; Harrison et al. 2020). Plants typically operate below their anatomical maximum by dynamically regulating stomatal aperture. Even though operational stomatal conductance determines the realized photosynthetic rate and water use efficiency, anatomical parameters are useful in that they set the range of stomatal function (de Boer et al. 2016) and are correlated with actual stomatal function under natural conditions (Murray et al. 2020). All else being equal, larger, more densely packed, but evenly spaced stomata increase gas exchange (Franks and Beerling 2009; Dow et al. 2014; Lehmann and Or 2015). Smaller stomata may also be able to respond more rapidly than larger stomata, proving the ability of leaves to track short-duration environmental change (Drake et al. 2013). Stomata are most often found only on the lower leaf surface (hypostomy), but they occur on both surfaces (amphistomy) in some species (Metcalfe and Chalk 1950; Parkhurst 1978; Mott et al. 1982). Amphistomatous leaves have a second parallel pathway from the substomatal cavities through the leaf internal airspace to sites of carboxylation in the mesophyll (Parkhurst 1978; Gutschick 1984). Thus, amphistomatous leaves have lower resistance to diffusion through the airspace, which increases the photosynthetic rate (Parkhurst and Mott 1990). If total stomatal and other conductances to CO<sub>2</sub> supply could be held constant, then an amphistomatous leaf will have a greater conductance than an otherwise identical hypostomatous leaf. The magnitude of the advantage depends on the resistance to diffusion through the internal airspace, which is variable among species.

The adaptive significance and ecological distribution of leaves with different stomatal anatomies is complex, and there is much yet to learn. Seed plants possess a wider range of stomatal anatomies than ferns and fern allies, which are restricted to having large stomata, at low density, only on the lower surface (de Boer et al. 2016). In general, trees and shrubs have greater stomatal density than herbs, but there is a lot of variation within growth forms depending on the ecological niche (Salisbury 1928; Kelly and Beerling 1995). A commonly observed trend is that leaves from higher-light environments tend to have greater stomatal density (Salisbury 1928; Mott et al. 1982; Gibson 1996; Smith et al. 1998; Jordan et al. 2014; Muir 2015; Bucher et al. 2017). This may explain why, perhaps counterintuitively, plants in dry environments tend to have more stomata. Drier habitats are more open, enabling plants with higher stomatal density to photosynthe-

size more when water is available but close stomata during drought (Liu et al. 2018). Over recent human history, stomatal density has tended to decline within species as atmospheric CO<sub>2</sub> concentrations have risen (Woodward 1987; Royer 2001). It is unclear whether most of this change is plastic or genetic, but the overall direction is consistent with the hypothesis that plants decrease gas exchange as CO<sub>2</sub> availability increases.

Stomatal ratio is a continuous measure of how stomata are deployed across leaf surfaces. The adaptive significance of variation in stomatal ratio is uncertain, but we have some clues based on the distribution of hypo- and amphistomatous leaves. Despite the fact that amphistomy can increase photosynthesis, most leaves are hypostomatous. Amphistomy should increase photosynthesis most under saturating-light conditions, where CO<sub>2</sub> supply limits photosynthesis. However, the light environment alone cannot explain why hypostomatous leaves predominate in shade plants (Muir 2019), suggesting that we need to understand the costs of upper stomata better. One factor may be increased vulnerability to pathogens. For example, upper stomata increase susceptibility to rust pathogens in *Populus* (McKown et al. 2014, 2019; Fetter et al. 2021). Amphistomy may also cause the palisade mesophyll to dry out under strong vapor pressure deficits (Buckley et al. 2015). Other hypotheses about the adaptive significance of stomatal ratio are discussed in Muir (2015) and Drake et al. (2019).

#### *Major Features of Stomatal Anatomical Macroevolution*

Two major features of stomatal anatomy have been recognized for decades, but we do not yet understand the evolutionary forces that generate and maintain them. We refer to these features as “inverse size-density scaling” and “bimodal stomatal ratio” (fig. 1). Inverse size-density scaling refers to the negative interspecific correlation between the size of the stomatal apparatus and the density of stomata (Weiss 1865; Franks and Beerling 2009; de Boer et al. 2016; Sack and Buckley 2016; Liu et al. 2021). Across species, leaves with smaller stomata tend to pack them more densely, but there is significant variation about this general trend (fig. 1*a*). Stomatal size and density determine the maximum stomatal conductance to CO<sub>2</sub> and water vapor but also take up space on the epidermis, which could be costly for both construction and maintenance. Natural selection should favor leaves that have enough stomata of sufficient size to supply CO<sub>2</sub> for photosynthesis. Hence, leaves with few small stomata and high photosynthetic rates do not exist because they would not supply enough CO<sub>2</sub>. Conversely, excess stomata or extra large stomata beyond the optimum may result in stomatal interference, where the CO<sub>2</sub> concentration gradient around one

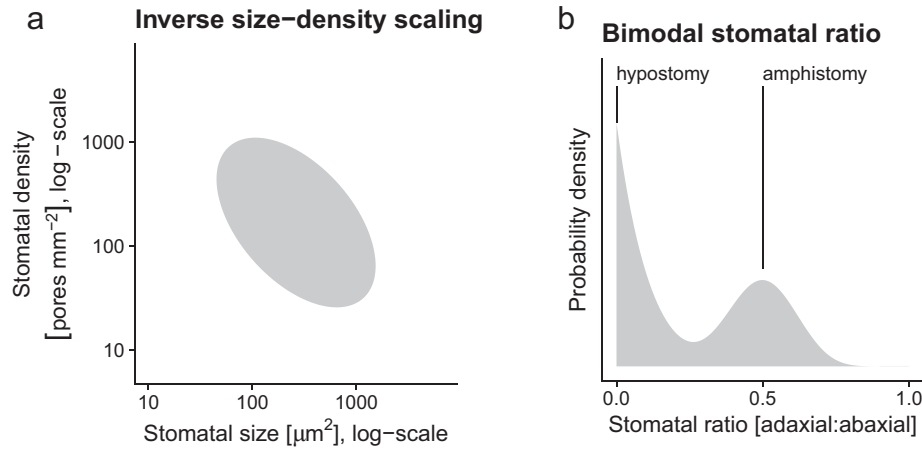


**Figure 1:** Two salient features of stomatal anatomy in flowering plants are the inverse relationship between stomatal size and density (*a*) and the bimodal distribution of stomatal ratio (*b*). At broad phylogenetic scales, species with smaller stomata on their leaves (*x*-axis, log scale) tend to have greater stomatal density (*y*-axis, log scale), but there is a lot of variation about the overall trend indicated by the gray ellipse. Hypostomatous leaves (stomatal ratio = 0) are more common than amphistomatous leaves, but within amphistomatous leaves the density of stomata on each surface tends to be similar (stomatal ratio  $\approx 0.5$ ), which we refer to as bimodal stomatal ratio.

stomate merges with that of its neighbor (Zeiger et al. 1987; Lehmann and Or 2015), incurs metabolic costs (Deans et al. 2020), and/or risks hydraulic failure (Henry et al. 2019). The distribution of stomatal size and density may therefore represent the combinations that ensure enough, but not too much, stomatal conductance. Franks and Beerling (2009) further hypothesized that the evolution of small stomata in angiosperms enabled increased stomatal conductance while minimizing the epidermal area allocated to stomata.

A striking feature of the interspecific variation in stomatal ratio is that trait values are not uniformly distributed but are strongly bimodal (fig. 1*b*). Bimodal stomatal ratio refers to the observation that the ratio of stomatal density on the adaxial (upper) surface to the density on the abaxial (lower) has distinct modes (fig. 1*b*). Amphistomy occurs most often in herbaceous plants from open, high-light habitats (Salisbury 1928; Mott et al. 1982; Gibson 1996; Smith et al. 1998; Jordan et al. 2014; Muir 2015, 2018; Bucher et al. 2017). Muir (2015) described bimodal stomatal ratio formally, but the pattern is apparent in earlier comparative studies of the British flora (see Peat and Fitter 1994, their fig. 1).

#### *Packing Limits, Developmental Integration, and Stomatal Anatomy*

Given the significance of stomata for plant function and global vegetation modeling (Berry et al. 2010), we would like to understand what factors constrain their anatomical variation. Here, we focus on interspecific variation in mean trait values rather than intraspecific variation. Pack-

ing constraints and developmental integration could explain inverse size-density scaling. The density and size of stomata on a planar leaf surface can be viewed as a packing problem where the total area allocated to stomata cannot exceed the total leaf area. This is a functional, or geometric, constraint because certain combinations of large size and high density are not physically possible. This functional constraint cannot explain why combinations of low density and small size are rare, but it may explain why stomatal size must decrease when density increases as the leaf runs out of space. The packing limit of functional stomata is less than the entire leaf area, but the exact value is unclear. The realized upper limit is close to one-third or one-half (de Boer et al. 2016; Sack and Buckley 2016; Liu et al. 2021) for the species' mean, not an individual leaf.

Guard cell size and spacing between stomata (the inverse of density) are developmentally intertwined because guard cells and epidermal pavement cells between stomata develop from the same meristem. Before guard cell meristemoids form via asymmetric cell division (Dow and Bergmann 2014), the size of guard and epidermal cells are influenced by meristematic cell volume and expansion. Evolutionary shifts in meristematic cell volume or expansion rate could cause both increased stomatal size and lower density because epidermal cells between stomata are larger (Brodrigg et al. 2013). For example, larger genomes increase meristematic cell volume (Šimová and Herben 2012), which sets a lower bound on final cell volume. Although different expansion rates in guard and epidermal pavement cells can reduce the correlation in their final size, the fact that species with larger genomes tend toward having larger stomata and lower density may indicate an effect of development

integration on stomatal anatomy (Beaulieu et al. 2008; Simonin and Roddy 2018; Roddy et al. 2020). Developmental integration in this case would not necessarily slow adaptive evolution if the main axes of selection were aligned with the developmental correlation. For example, if higher maximum stomatal conductance were achieved primarily by increasing stomatal density and decreasing stomatal size, as proposed by Franks and Beerling (2009), then developmental integration might accelerate the response to selection compared with a case where stomatal size and density are completely independent.

Muir (2015) showed that bimodality can arise adaptively if fitness optima are restricted to separate regimes. Specifically, if either the fitness costs or benefits of allocating additional stomata to the upper surface are nonlinear with the correct curvature, then there are distinct “hypostomatous” and “amphistomatous” regimes. An alternative hypothesis is that stomatal traits on the ab- and adaxial surfaces are developmentally integrated because stomatal development is regulated the same way on each surface. In hypostomatous leaves, stomatal development is turned off on the adaxial surface. In amphistomatous leaves, stomatal development proceeds on both surfaces, but evolutionary changes in stomatal development affect traits on both surfaces because they are tethered by a shared developmental program. This is a developmental constraint because the fact that stomatal development is the same on each surface constrains the type of variation available for selection. Developmental integration would lead to a bimodal trait distribution because leaves would either be hypostomatous (stomatal ratio equal to zero) or have similar densities on each surface (stomatal ratio of approximately 0.5). To our knowledge, this hypothesis has not been put forward in the literature.

#### *Hypotheses and Predictions*

The overarching question is whether major features of stomatal anatomy in terrestrial angiosperms are consistent with packing constraints and/or developmental integration mediated by cell size. Since stomata on both surfaces of amphistomatous leaves are subject to the same functional and developmental constraints, if these constraints are most important we predict similar patterns of trait covariation on abaxial and adaxial surfaces. Conversely, if traits covary differently on each surface it would indicate that stomatal anatomical traits can evolve independently and selection against generally maladaptive trait combinations shapes covariation. Analogously, variation in the genetic correlation and interspecific divergence of sexually dimorphic traits in dioecious species demonstrate that integration is not fixed and can be modified by selection (Barrett and Hough 2013). We framed specific hy-

potheses and predictions around how functional or developmental constraints might explain either inverse size-density scaling or bimodal stomatal ratio.

*Inverse Size-Density Scaling.* Both packing limits and developmental integration could contribute to inverse size-density scaling. If limits on the fraction of epidermal area occupied by stomata constrains the combinations of stomatal size and density that are evolutionarily accessible, then we predict that evolutionary divergence in stomatal size and/or density will decrease as the fraction of epidermal area occupied by stomata increases. Furthermore, if divergence slows as epidermal area occupied by stomata because of a packing limit, it should slow down the same way for both ab- and adaxial surfaces.

The second hypothesis is that cell size mediates developmental integration between stomatal size and density. If developmental integration is the primary reason for inverse size-density scaling, then amphistomatous leaves will exhibit identical size-density scaling on each surface. If the stomatal size and density scale differently on each surface, this implies that they can evolve independently and that selection against generally maladaptive trait combinations shapes their covariance. Furthermore, we predicted that divergence in genome size, which is strongly associated with meristematic cell volume (Šímová and Herben 2012), would covary with stomatal size and density similarly on each surface.

*Bimodal Stomatal Ratio.* If the developmental integration hypothesis is correct, it also implies that stomatal size and density will diverge in concert on each surface because the developmental function is fixed. Therefore, we predict that divergence of stomatal traits on one surface will be isometric with divergence in stomatal traits on the other surface. This type of developmental integration limits the expression of variation and could give rise to a bimodal stomatal ratio. Suppose that in hypostomatous leaves, stomatal development is completely suppressed. In amphistomatous leaves, stomatal development proceeds identically on each surface because the developmental function is identical. This would lead to a tendency for equal density on each surface.

We formalized these hypotheses into a mathematical framework to derive quantitative predictions that we tested in a phylogenetic comparative framework by compiling stomatal anatomy data from the literature for a broad range of flowering plants.

#### **Material and Methods**

Unless otherwise mentioned, we performed all data wrangling and statistical analyses in R version 4.2.2 (R Core

Team 2022). Source code is publicly available on GitHub (<https://github.com/cdmuir/stomata-independence>) and archived in the Dryad Digital Repository (<https://doi.org/10.5061/dryad.0rxwdb42>; Muir et al. 2022).

*Theory: Divergence With and Without  
Developmental Constraint*

Developmental integration could shape patterns of phenotypic macroevolution, but a major hindrance to progress is that verbal models do not make precise quantitative predictions that distinguish it from alternatives. An advantage of testing developmental integration in stomata is that their development is well studied (Bergmann and Sack 2007; Dow and Bergmann 2014; Sack and Buckley 2016). We can leverage that knowledge to build a developmental function and derive equations for phenotypic (co)variance caused by developmental integration. If observed patterns of evolution are inconsistent with developmental integration, theory may also help identify which parameters lead to developmental disintegration. We combined and extended stomatal development models to predict how stomatal density and length would diverge if stomatal development were constrained and how those predictions would change if stomatal development were unconstrained. We summarize our methods verbally here and direct readers interested in the mathematical details to the supplemental PDF. A graphical summary is provided in figure S3. We imposed constraint by assuming the stomatal developmental function is constrained. The developmental function maps cell size prior to differentiation onto stomatal size and density using two parameters. The first parameter describes how cell volume is apportioned between epidermal cells and guard cell meristemoids during asymmetric cell division (Dow and Bergmann 2014). The second parameter is a stomatal index (Salisbury 1928; Sack and Buckley 2016), determined by amplifying and spacing divisions after asymmetric cell division (Dow and Bergmann 2014). When these parameters are fixed, divergence in stomatal size and density is determined by divergence in meristematic cell volume and expansion prior to asymmetric division. We relaxed this constraint by treating parameters of the developmental function as random variables that can diverge between species. We used random variable algebra to derive predicted (co)variance in divergence between stomatal length and density (for key random variable algebra theorems, see Lynch and Walsh 1998).

*Data Synthesis*

We searched the literature for studies that measured stomatal density and stomatal size, either guard cell length or stomatal pore length, for both abaxial and adaxial leaf

surfaces. In other words, we did not include studies unless they reported separate density and size values for each surface. We did not record leaf angle because it is typically not reported, but we presume that for the vast majority of taxa the abaxial is the lower surface and the adaxial is the upper surface. This is reversed in resupinate leaves, but to the best of our knowledge our synthesis did not include resupinate leaves. None of the species with resupinate leaves listed by Chitwood et al. (2012) are in our data set. We refer to guard cell length as stomatal length and converted stomatal pore length to stomatal length assuming that guard cell length is twice pore length (Sack and Buckley 2016). Table 1 lists anatomical traits and symbols. Abaxial traits are subscripted with “ab”; adaxial traits are subscripted with “ad.”

Data on stomatal anatomy are spread over a disparate literature, and we have not attempted an exhaustive synthesis of amphistomatous leaf stomatal anatomy. We began our search by reviewing articles that cited key studies of amphistomy (Parkhurst 1978; Mott et al. 1982; Muir 2015). We supplemented these by searching Clarivate Web of Science for “guard cell length” because most studies that report guard cell length also report stomatal density, whereas the reverse is not true. We identified additional studies by reviewing the literature cited of articles we found and through opportunistic discovery. The final data set contained 5,104 observations of stomatal density and length from 1,242 taxa and 38 primary studies (table S5). However, many of these data were excluded if taxonomic name and phylogenetic placement could not be resolved (see below). Finally, we included some unpublished data. Stomatal size data were collected on grass species described in Pathare et al. (2020). We also included unpublished data on 14 amphistomatous wild tomato species (*Solanum* sect. *Lycopersicum* and sect. *Lycopersicoides*) grown in pots under outdoor summer Mediterranean conditions (C. D. Muir, J. Galmés, and M. À. Conesa, unpublished data). We took ab- and adaxial epidermal

**Table 1:** Stomatal anatomical traits with mathematical symbol, description, and scientific units

Symbol	Definition	Unit
$D_{ab}$	Stomatal density on abaxial (lower) surface	pores $\text{mm}^{-2}$
$D_{ad}$	Stomatal density on adaxial (upper) surface	pores $\text{mm}^{-2}$
$f_s$	Fraction of epidermal area allocated to stomata	unitless
$L_{ab}$	Guard cell length on abaxial (lower) surface	$\mu\text{m}$
$L_{ad}$	Guard cell length on adaxial (upper) surface	$\mu\text{m}$

imprints using clear nail polish of the midportion of the lamina away from major veins on the terminal leaflet of the youngest, fully expanded leaf from one to five replicates per taxon. With a bright-field light microscope, we counted stomata in three 0.571-mm<sup>2</sup> fields of view and divided by the total area to estimate density. We measured the average guard cell length of 60 stomata, 20 per field of view, to estimate stomatal size. The data set is publicly available as an R package `ropenstomata` (<https://github.com/cdmuir/ropenstomata>). We collected data on genome size from the Angiosperm DNA C-values database (Leitch et al. 2019; Pellicer and Leitch 2020). When multiple ploidy levels were available for a taxon, we chose the lowest one for consistency.

#### *Phylogenetically Independent Contrasts*

We generated an ultrametric bifurcating phylogeny of 638 taxa by resolving and removing ambiguous taxonomic names, placing taxa on the GBOTB.extended megatree of seed plants (Zanne et al. 2014; Smith and Brown 2018), and resolving polytomies using published sequence data. Divergence times in this phylogeny are based on extensive fossil calibration (for further details, see Magallón et al. 2015; Smith and Brown 2018). The complete methodology is described in the supplemental PDF.

From this phylogeny, we extracted 236 phylogenetically independent taxon pairs (table S1). A fully resolved bifurcating four-taxon phylogeny can have two basic topologies: ((A, B), (C, D)) or ((A, B), C), D)). Taxon pairs include all comparisons of A with B and C with D in each four-taxon clade. We extracted pairs using the `extract_sisters()` function in the R package `diverge` (ver. 2.0.4; Anderson and Weir 2021) and custom scripts (see source code). Taxon pairs are the most closely related pairs in our data set, but they are mostly not sister taxa in the sense of being the two most closely related taxa in the tree of life. For each pair we calculated phylogenetically independent contrasts (Felsenstein 1985) as the difference in the log<sub>10</sub>-transformed trait value (for a similar approach, see Beaulieu et al. 2008). Contrasts are denoted as  $\Delta\log(\text{trait})$ . We log-transformed traits for normality because like many morphological and anatomical traits, they are strongly right skewed. Log transformation also helps compare density and length, which are measured on different scales, because log-transformed values quantify proportional rather than absolute divergence.

#### *Parameter Estimation*

All hypotheses make predictions about trait (co)variance matrices or parameters derived from them (see the supplemental PDF and subsections below). Within- and

among-species covariation is a hallmark of developmental integration (Armbruster 1988), but other evolutionary processes also lead to covariance. Distinguishing between them requires deriving predictions and testing whether observed covariance is consistent with one hypothesis or another. We estimated the  $4 \times 4$  covariance matrix of phylogenetically independent contrasts between log-transformed values of  $\Delta\log(D_{ab})$ ,  $\Delta\log(D_{ad})$ ,  $\Delta\log(L_{ab})$ , and  $\Delta\log(L_{ad})$  using a distributional multiresponse robust Bayesian approach. See table 1 for variable definitions. We denote variances as  $\text{Var}[\Delta\log(\text{trait})]$  and covariances as  $\text{Cov}[\Delta\log(\text{trait}_1), \Delta\log(\text{trait}_2)]$ . We used a multivariate  $t$  distribution rather than a normal distribution because estimates using the former are more robust to exceptional trait values (Lange et al. 1989). We also estimated whether the variance in trait divergence increases with time. Under many trait evolution models (e.g., Brownian motion), interspecific variance increases through time. To account for this, we included time since taxon-pair divergence as an explanatory variable affecting the trait covariance matrix.

For the packing limit hypothesis, we tested whether the variance in stomatal trait divergence,  $\text{Var}[\Delta\log(\text{trait})]$ , decreases as stomatal allocation increases. The fraction of epidermal area allocated to stomata ( $f_s$ ) is the product of stomatal density and area occupied by a stomatal apparatus. Because guard cell shape is similar in most plant lineages except grasses, the area can be well approximated from guard cell length as  $A = jL^2$ , where  $j = 0.5$  for most species with kidney-shaped guard cells and  $j = 0.125$  for grasses with dumbbell-shaped guard cells (Sack and Buckley 2016). For each contrast, we calculated the average  $f_s$  on each surface between those two taxa for use as our explanatory variable. The statistical model allowed the effect of  $f_s$  on  $\text{Var}[\Delta\log(\text{trait})]$  to vary between traits and leaf surfaces. We also included time since taxon-pair divergence as an explanatory variable and used a multivariate  $t$  distribution as described above.

We fit all models in Stan (ver. 2.29; Stan Development Team 2022) using the R package `brms` (ver. 2.17.0; Bürkner 2017, 2018) with a `CmdStanR` backend (ver. 0.5.2; Gabry and Češnovar 2022). It ran on two parallel chains for 1,000 warm-up iterations and 1,000 sampling iterations. All parameters converged ( $\hat{R} \approx 1$ ), and the effective sample size from the posterior exceeded 1,000 (Vehtari et al. 2021). We used the posterior median for point estimates and calculated uncertainty with the 95% highest posterior density (HPD) interval from the posterior distribution.

#### *Hypothesis Testing*

*Does Divergence Slow as Epidermal Space Fills?* We tested the packing limit hypothesis by estimating whether the

fraction of epidermal area allocated to stomata ( $f_s$ ) affects  $\text{Var}[\Delta \log(\text{trait})]$  for each trait and leaf surface. If there is an upper bound on  $f_s$ , we predict the effect of  $f_s$  on  $\text{Var}[\Delta \log(\text{trait})]$  will be less than zero. Specifically, the 95% HPD intervals should not include zero. Furthermore, the coefficient should be the same on each surface, so the 95% HPD intervals for difference should encompass zero.

#### *Is Size-Density Scaling the Same on Both Leaf Surfaces?*

We tested whether the covariance between divergence in stomatal length and stomatal density on each leaf surface is the same. If size and density are developmentally integrated, we predict that the covariance matrices will not be significantly different. Specifically, the 95% HPD intervals of the difference in covariance parameters should not include zero if

$$\text{Var}[\Delta \log(D_{ab})] \neq \text{Var}[\Delta \log(D_{ad})], \quad (1)$$

$$\text{Var}[\Delta \log(L_{ab})] \neq \text{Var}[\Delta \log(L_{ad})], \quad (2)$$

$$\text{Cov}[\Delta \log(L_{ab}), \Delta \log(D_{ab})] \neq \text{Cov}[\Delta \log(L_{ad}), \Delta \log(D_{ad})]. \quad (3)$$

*Do Abaxial and Adaxial Stomatal Traits Evolve Isometrically?* If stomatal traits on each surface are developmentally integrated, then divergence in the trait on one surface should result in a 1:1 (isometric) change in the trait on the other surface. Furthermore, there should be relatively little variation away from a 1:1 relationship. Conversely, if traits can evolve independently, then the change in the trait on one surface should be uncorrelated with changes on the other. We tested for isometry by estimating the standardized major axis (SMA) slope of divergence in the abaxial trait against divergence in the adaxial trait for both stomatal length and stomatal density. If change on each surface is isometric, then the HPD intervals for the slope should include 1. We used the coefficient of determination,  $r^2$ , to quantify the strength of integration, where a value of 1 is complete integration and a value of 0 is complete disintegration.

## Results

### *Theory: From Developmental Integration to Disintegration*

We asked how divergence in stomatal length and density would covary if the developmental function were constrained and compared it to their divergence when the developmental function can evolve. When the developmental function is constrained, this means that allocation to guard cell meristemoids during asymmetric division and

stomatal index are fixed (for a mathematical description, see the supplemental PDF). Under these assumptions, divergence in stomatal length and density is mediated entirely by divergence in meristematic cell volume and expansion prior to differentiation. Developmental integration is strong because divergence in density is perfectly negatively correlated with divergence in size. In contrast, stomatal length and density can diverge independently when the developmental function is not fixed. Divergence in asymmetric cell division affects stomatal size independently of density; divergence in stomatal index affects stomatal density independently of size. Divergence in the developmental function causes developmental disintegration because stomatal density and size can diverge independently. Developmental integration is minimal when asymmetric cell division and/or stomatal index diverge more than meristematic cell volume and expansion. The three main conclusions are that (1) developmental constraint leads to developmental integration; (2) different (co)variance in divergence of stomatal length and density on each surface implies the developmental function is not fixed; and (3) divergence in different components of the developmental function affect stomatal length and density differently. See the supplemental PDF and table S4 for more a complete derivation and detailed predictions.

### *Empirical Results*

The variance in trait divergence decreases as the fraction of epidermal area allocated to stomata,  $f_s$ , increases (figs. 2, S1). The effect of  $f_s$  was strongest for adaxial stomatal density ( $D_{ad}$ ) and 95% HPD intervals did not overlap zero for three of four comparisons (table S2). Variance in divergence for  $D_{ad}$  declined more rapidly with  $f_s$  than did that for abaxial stomatal density ( $D_{ab}$ ; difference [95% HPD interval] in slope, log-link scale:  $-10.7$  [ $-17.2$  to  $-4.2$ ]). Variance in length divergence declined similarly with  $f_s$  on both surfaces (difference [95% HPD interval] in slope, log-link scale:  $-2.8$  [ $-9.6$  to  $4$ ]).

Stomatal length negatively covaries with stomatal density similarly on both surfaces, but on the adaxial surface there are many more taxa that have low stomatal density and small size compared with the abaxial surface (fig. 3). In principle, this pattern could arise either because size-density covariance differs or the variance in adaxial stomatal density increases faster than that for abaxial stomatal density. The interspecific variance increases with time since divergence for all traits (table S3). For consistency, we therefore report estimates conditional on time since divergence set to zero. Across pairs, we estimate that the covariance between size and density is similar. The median estimate is  $\text{Cov}[\Delta \log(L_{ad}), \Delta \log(D_{ad})] - \text{Cov}[\Delta \log(L_{ab}), \Delta \log(D_{ab})] = 3.18 \times 10^{-4}$ , but zero is within the range

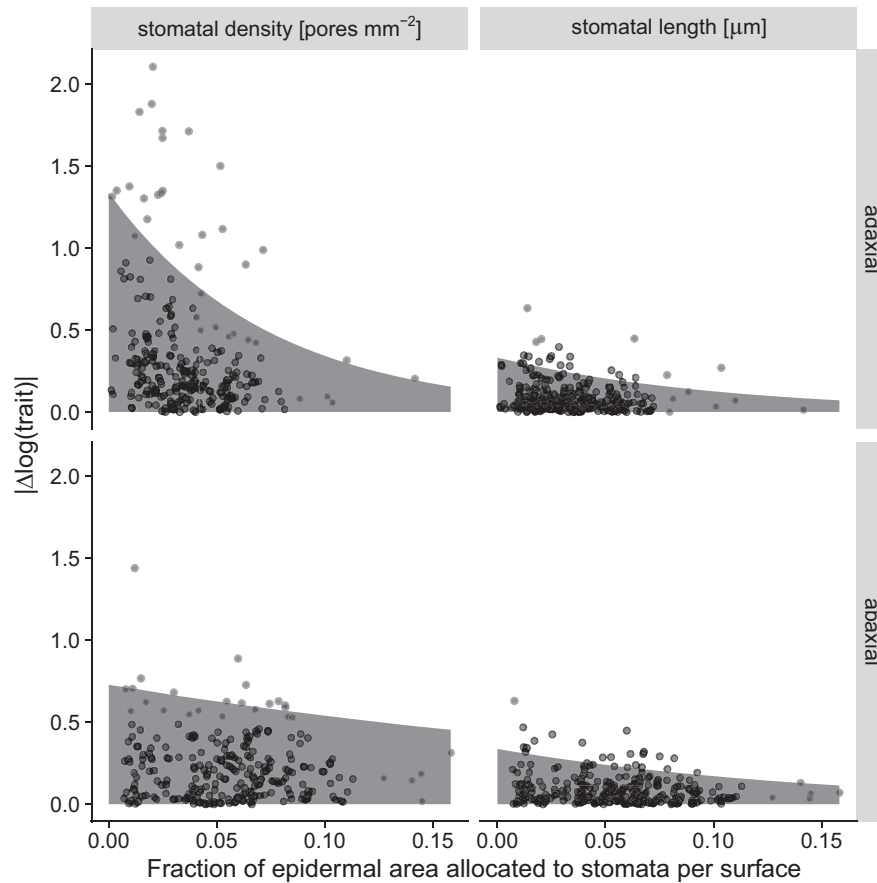


**Figure 2:** Evolutionary divergence slows down as epidermal space fills up. This pattern is consistent with functional constraints (packing limits) constraining evolution, but only when stomata occupy a large fraction of epidermal area. The shaded area in each facet indicates the estimate of where 95% of the 236 phylogenetically independent contrasts fall as a function of the fraction of epidermal area allocated to stomata per surface. Each point is the absolute value of  $\Delta\log(\text{trait})$  for stomatal density (left facets) or length (right facets) on the adaxial (upper facets) and abaxial (lower facets) surface. The fraction of epidermal area allocated to stomata is the average value per surface between the two taxa in each contrast. Divergence in anatomical traits is more variable when stomata occupy a smaller area, especially for adaxial stomatal density (upper left facet). See table S2 for all parameter estimates and confidence intervals.

of uncertainty (95% HPD interval:  $-3.85 \times 10^{-3}$  to  $4.26 \times 10^{-3}$ ). However, the variance in adaxial stomatal density is significantly greater than the abaxial stomatal density (fig. 4). We estimate that  $\text{Var}[\Delta\log(D_{\text{ad}})]$  is  $4.00 \times 10^{-2}$  (95% HPD interval:  $1.42 \times 10^{-2}$  to  $7.07 \times 10^{-2}$ ) greater than  $\text{Var}[\Delta\log(D_{\text{ab}})]$ . The variance in stomatal length was similar for both surfaces, with an estimate of  $-4.54 \times 10^{-4}$  (95% HPD interval:  $-1.67 \times 10^{-3}$  to  $7.45 \times 10^{-4}$ ).

We analyzed a smaller set of 79 contrasts with data on both genome size and stomatal anatomy. Consistent with previous studies (Beaulieu et al. 2008; Jordan et al. 2015; Simonin and Roddy 2018), increased genome size was associated with increased stomatal length on both surfaces (fig. S2). The association between genome size and stomatal density was negative, as expected, but weaker. Only the

slope for adaxial stomatal density was significantly less than zero (fig. S2).

Stomatal density on each surface is less integrated than stomatal length. The relationship between stomatal density on each leaf surface is visually more variable than that for stomatal length (fig. 5). This pattern occurs because the slope and strength of integration for stomatal density on each surface is much weaker than that for stomatal length. The SMA slope between  $\Delta\log(D_{\text{ad}})$  and  $\Delta\log(D_{\text{ab}})$  is less than 1 (estimated slope = 0.742; 95% HPD interval: 0.619 to 0.883), and the strength of association is weakly positive (estimated  $r^2 = 0.113$ ; 95% HPD interval: 0.0431 to 0.205; fig. 6). In contrast, the relationship between  $\Delta\log(L_{\text{ad}})$  and  $\Delta\log(L_{\text{ab}})$  is isometric (estimated slope = 1.03; 95% HPD interval: 0.955 to 1.12) and strongly

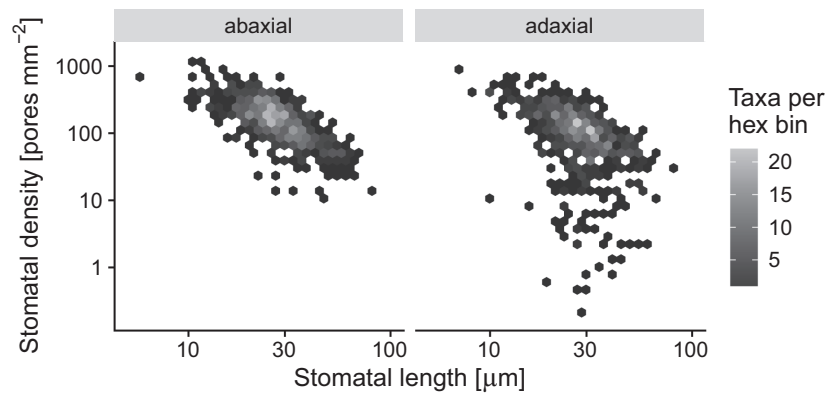


**Figure 3:** Inverse size-density scaling differs between the surfaces of amphistomatous leaf, indicating different phenotypic constraints. The panels show the relationship between stomatal length ( $x$ -axis) and stomatal density ( $y$ -axis) on a log-log scale for values measured on the abaxial leaf surface (*left*) and the adaxial leaf surface (*right*) across 638 taxa.

positive (estimated  $r^2 = 0.762$ ; 95% HPD interval: 0.691 to 0.82; fig. 6).

### Discussion

Functional and developmental constraints may slow adaptation by preventing traits from evolving independently toward a multivariate phenotypic optimum. An alternative view is that phenotypic evolution is limited primarily because most phenotypes are maladaptive and selected against, sometimes referred to as selective constraint. In this study, we took advantage of the fact that amphistomatous leaves produce stomata on both abaxial (usually lower) and adaxial (usually upper) surfaces. Packing limits, a functional constraint, and developmental integration should result in similar (co)variance in divergence of stomatal traits on each surface (see the supplemental PDF), whereas differing selective pressures for each surface would lead to different patterns of divergence. Although some patterns of trait (co)variance are compatible with packing limits or developmental integration (see below), independent evolution of stomatal density on each surface across flowering plants is notably inconsistent with these constraints. We therefore conclude that selection against generally maladaptive trait combinations plays a major role in the evolution of stomata and possibly other ecologically important traits. It should not be surprising that stomatal traits respond to natural selection, but it is nevertheless plausible that some stomatal trait combinations that would have high fitness are precluded by nonadaptive constraints. Our results challenge these nonadaptive explanations, especially for stomatal density.

Neither packing limits nor developmental integration were sufficient to explain two major patterns of divergence in stomatal traits (fig. 1). Although evolutionary di-

vergence slowed as the allocation to stomata  $f_s$  increased, the effect of  $f_s$  was different on each surface (figs. 2, S1; table S2). The contrasting pattern of divergence on each surface is inconsistent with a common packing limit and suggests instead that a different range of adaptive stomatal trait combinations on the lower and upper leaf surface. Contrary to the developmental integration hypotheses, the greater variance in stomatal density compared with length on the adaxial surface indicates that density is more labile on this surface, although traits on each surface are not completely decoupled (figs. 4, 6; table S3). Consistent with the developmental integration hypotheses, divergence in stomatal length on each surface evolves isometrically at the same rate, suggesting that guard cell dimensions may not be able to evolve independently on each surface (fig. 6). The evolutionary lability of stomatal density, despite constraints on size, show that inverse size-density scaling and bimodal stomatal ratio cannot be attributed entirely to developmental integration. Combinations of small stomata and low density that are not found on the abaxial surface are found on the adaxial surface, indicating that these rare trait combinations are developmentally accessible.

While phylogenetic comparisons usually cannot prove that phenotypic variation is adaptive, ruling out alternative hypotheses as the sole explanation is an important step toward quantifying the relative importance of adaptation in macroevolution (McGhee 1999; Olson 2019). Establishing that traits can evolve quasi-independently is necessary but not sufficient to show that selection is the primary process shaping phenotypic evolution. Packing limits and developmental integration may bias phenotypic evolution, even if they do not preclude certain stomatal trait combinations. Therefore, future research will need to combine stomatal developmental (dis)integration

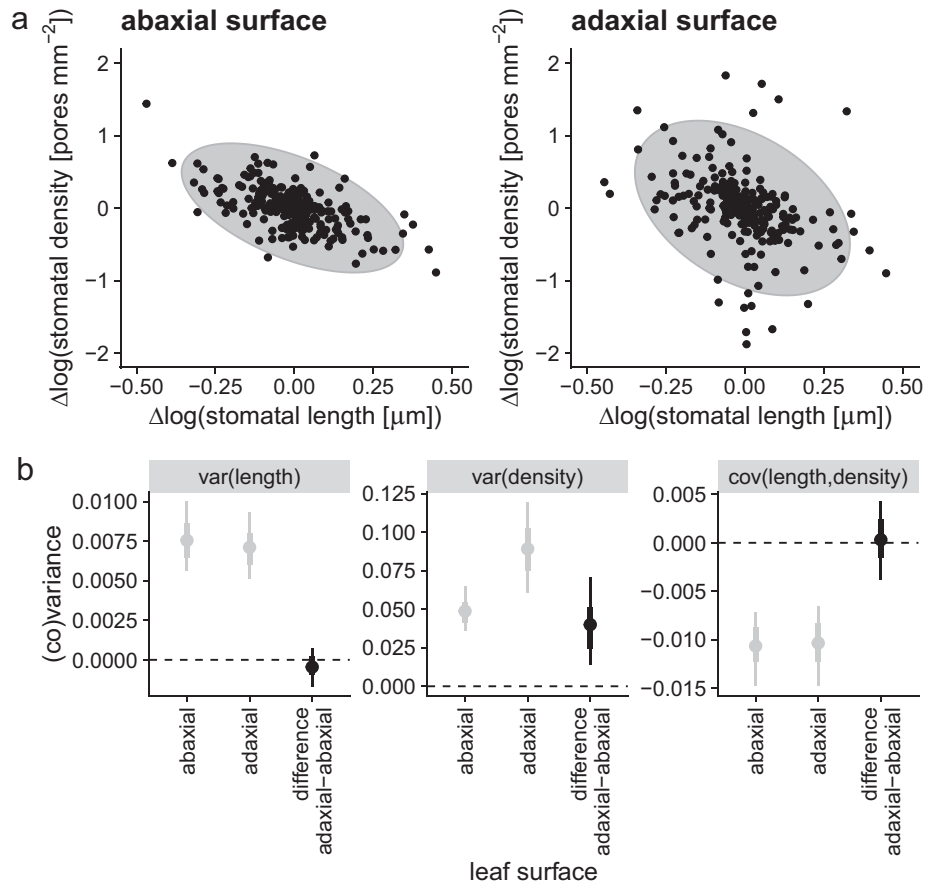


**Figure 4:** Greater overall phenotypic constraint on abaxial stomatal anatomy is evinced by more variable evolutionary divergence in adaxial stomatal density, but covariance between density and length is similar on both surfaces. *a*, Data from 236 phylogenetically independent contrasts of change in  $\log(\text{stomatal length})$  ( $x$ -axis) and  $\log(\text{stomatal density})$  ( $y$ -axis) for abaxial (*left*) and adaxial (*right*) leaf surfaces. Each contrast is shown by black points, and every contrast appears on both panels. Gray ellipses are the model-estimated 95% covariance ellipses. The negative covariance is similar for both surfaces, but the breadth in the  $y$  direction is larger for adaxial traits, indicating greater evolutionary divergence in  $\log(\text{stomatal density})$ . *b*, Parameter estimates (points), 66% (thick lines), and 95% highest posterior density (HPD) intervals for estimates of trait (co)variance. Gray points and lines represent ab- and adaxial values; black points and lines represent the estimated difference in (co)variance between surfaces. Only the variance for stomatal density (*middle*) is significantly greater for the adaxial surface (95% HPD interval does not overlap the dashed line at zero). Reported parameter estimates are conditioned on zero time since divergence between taxa (see “Results”).

with biophysical models of how stomatal anatomy would vary adaptively (Olson and Arroyo-Santos 2015). Although these questions and approaches apply to any phenotype, stomata will be a useful trait because of their ecological significance and broad application to most land plants.

#### *Do Packing Limits and Developmental Integration Lead to Inverse Size-Density Scaling?*

Stomata cannot occupy more than the entire leaf surface, but realistically there is probably an upper packing limit below this hard bound. If this packing limit drives inverse size-density scaling, we should observe that divergence in stomatal size and density decrease as this limit is ap-

proached. Near the limit, large changes that reduce  $f_s$  are possible, but changes that increase  $f_s$  must be small so as not to exceed the limit. Furthermore, the same packing limit should apply to both ab- and adaxial leaf surfaces. Although we observe that divergence decreases with  $f_s$ , the relationship is not the same on both surfaces (figs. 2, S1; table S2). This implies that other factors constrain stomatal size and density before they approach a packing limit.

If meristematic cell volume and expansion integrate stomatal size and density (Brodribb et al. 2013), then we predicted that inverse size-density scaling would evolve with the same (co)variance for both ab- and adaxial leaf surfaces (see the supplemental PDF). Contrary to this prediction, there are many combinations of stomatal density

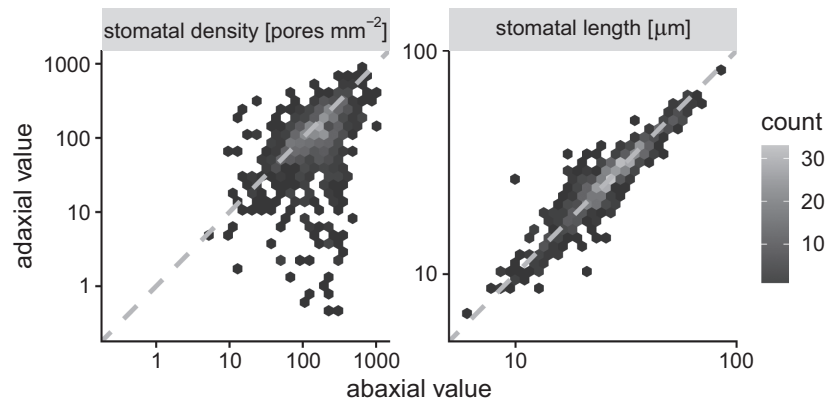


**Figure 5:** Stomatal density on each surface is less constrained (lower correlation) than stomatal length (higher correlation). Relationship between stomatal density and length on each leaf surface in a synthesis of amphistomatous leaf traits across 638 taxa. The panels show the relationship between the abaxial trait value ( $x$ -axis) and the adaxial trait value ( $y$ -axis) on a log-log scale for stomatal density (*left*) and stomatal length (*right*). The dashed line in across the middle is the 1:1 line for reference.

( $D_i$ ) and length ( $L_i$ ) found on adaxial leaf surfaces that are absent from abaxial leaf surfaces (fig. 3). In principle, the different relationship between traits on each surface could be caused by different evolutionary variance in stomatal density ( $\text{Var}[\Delta \log(D_{ab})] \neq \text{Var}[\Delta \log(D_{ad})]$ ) and/or covariance ( $\text{Cov}[\Delta \log(L_{ab}), \Delta \log(D_{ab})] \neq \text{Cov}[\Delta \log(L_{ad}), \Delta \log(D_{ad})]$ ) on each surface. However, the covariance relationship between density and length is similar on each surface, whereas the evolutionary variance in adaxial stomatal density is significantly higher than that for abaxial density ( $\text{Var}[\Delta \log(D_{ab})] < \text{Var}[\Delta \log(D_{ad})]$ ; fig. 4). Given that the average stomatal length is usually about the same on each surface (see below), these results imply that plants can often evolve stomatal densities on each surface without a concomitant change in size. Based on our theoretical analysis, we interpret these results to mean that cell divisions affecting stomatal index are less evolutionarily constrained than the asymmetric cell division preceding the guard cell meristemoid (fig. S3; table S4).

The disintegration of stomatal size and density on adaxial leaf surfaces implies that the inverse size-density scaling on abaxial surfaces (Weiss 1865; Franks and Beerling 2009; de Boer et al. 2016; Sack and Buckley 2016; Liu et al. 2021) is not a developmental fait accompli. The lability of  $D_{ad}$  may explain why there is so much putatively adaptive variation in the trait along light gradients (Muir 2018) and in coordination with other anatomical traits that vary among precipitation habitats (Pathare et al. 2020). There may appear to be a tension between our results and recent findings that genome size, which is strongly correlated with meristematic cell volume (Šímová and Herben 2012), correlates strongly with mature guard cell size as well as the size and packing density of mesophyll cells (Roddy et al. 2020; Théroux-Rancourt et al. 2021). How-

ever, most plant species are far from their minimum cell size, as determined by genome size (Roddy et al. 2020; fig. 3). Genome size explains 31%–54% of the variation in stomatal density across the major groups of terrestrial plants (Simonin and Roddy 2018), but there is huge variation in stomatal density and stomatal length in angiosperms with rather similar genome size (see fig. 2 in Simonin and Roddy 2018). Genome size, a proxy for meristematic cell volume, is more strongly related to stomatal size than density (fig. S2). Yet the decoupling of size and density on the adaxial surface suggests that meristematic cell volume is probably not a strong constraint on the final size of epidermal pavement and guard cells because of different division and expansion rates after the asymmetric cell division stage. A possible resolution is that meristematic cell volume limits the range of variation in species with exceptionally large genomes, but most species can modify stomatal size and density independently of each other to optimize photosynthesis (Jordan et al. 2015; Simonin and Roddy 2018; Roddy et al. 2020; Théroux-Rancourt et al. 2021).

#### *Does Developmental Integration Lead to Bimodal Stomatal Ratio?*

We predicted that if abaxial and adaxial stomata are developmentally integrated, then we should observe a strong isometric relationship between trait divergence on each surface. Consistent with this prediction, divergence in stomatal length on each surface is isometric (SMA slope = 1.03) and strongly associated ( $r^2 = 0.762$ ; fig. 6). In contrast, divergence in stomatal density on each surface was not isometric (SMA slope = 0.742) and much less integrated ( $r^2 = 0.113$ ; fig. 6). Since average stomatal density on each surface can evolve quasi independently, a wide

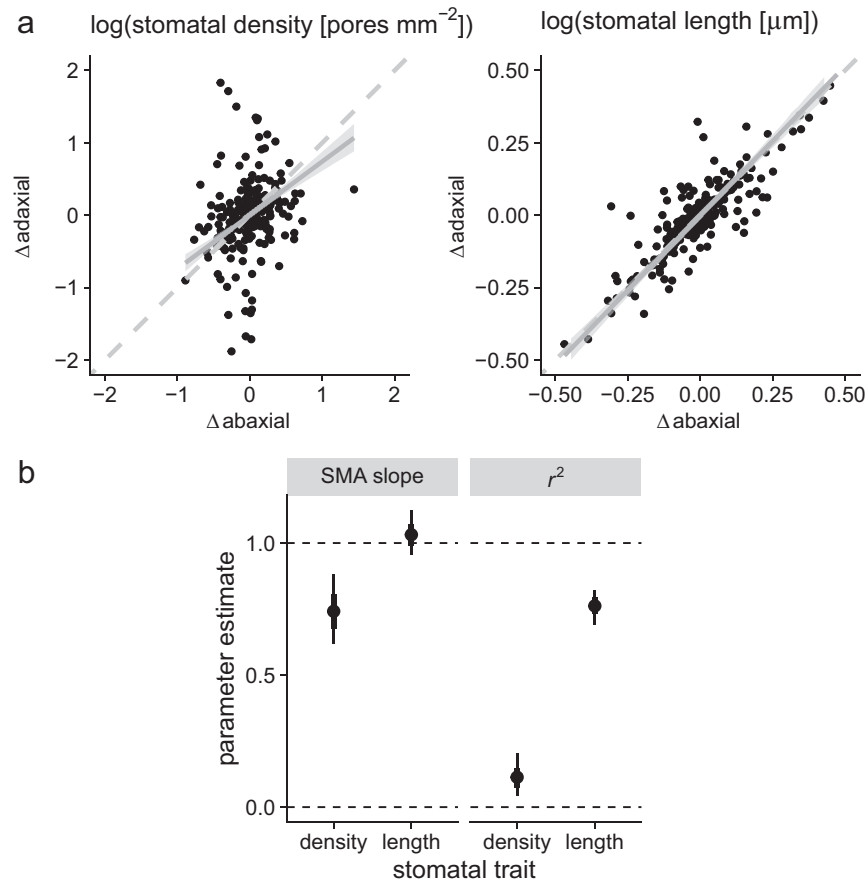


**Figure 6:** Developmental integration in stomatal length is much stronger than stomatal density between the surfaces of amphistomatous leaves. *a*, Data from 236 phylogenetically independent contrasts of change in the abaxial trait value ( $x$ -axis) against change in the adaxial trait value ( $y$ -axis) for  $\log(\text{stomatal density})$  (*left*) and  $\log(\text{stomatal length})$  (*right*). Each contrast is shown by black points, and every contrast appears on both panels. Dashed gray lines are 1:1 lines for reference. Solid gray lines and ribbon the fitted standardized major axis (SMA) slope and 95% highest posterior density (HPD) interval. *b*, The SMA slope (*left*) is significantly less than 1 (isometry, top dashed line) for density but very close to isometric for length. The coefficient of determination ( $r^2$ ; *right*) is also much greater for length than density. The points are parameter estimates with 66% (thick lines) and 95% HPD intervals. Reported parameter estimates are conditioned on zero time since divergence between taxa (see “Results”).

variety of stomatal ratios are developmentally possible. The stomatal developmental function is not constrained to be identical on each surface. If natural selection favored an intermediate stomatal ratio between modes, developmental processes should not constrain the expression of genetic variation to achieve it. This supports the hypothesis that the bimodal stomatal ratio pattern (Muir 2015) arises because natural selection rarely favors intermediate trait values, not because intermediate values are developmentally inaccessible.

#### *Limitations and Future Research*

The ability of adaxial stomatal density to evolve independently of stomatal size and abaxial stomatal density is not consistent with packing limits or developmental integra-

tion as the primary cause leading to inverse size-density scaling or bimodal stomatal ratio. However, there are two major limitations of this study that should be addressed in future work. First, while  $D_{\text{ab}}$  can diverge independently of other stomatal traits globally, we cannot rule out that developmental integration is important in some lineages. Developmental constraints are often localized to particular clades but are not universal (Maynard Smith et al. 1985). For example, Berg’s rule observes that vegetative and floral traits are often developmentally integrated, but integration can be broken when selection favors flowers for specialized pollination (Berg 1959, 1960; Conner and Lande 2014). Other traits evince developmental modularity, such as the independent evolution of leaf and petal venation (Roddy et al. 2013). Analogously, developmental integration between stomatal anatomical traits could

evolve in some lineages, due to selection or other evolutionary forces, but become less integrated in other lineages. For example,  $D_{ab}$  and  $D_{ad}$  are positively genetically correlated in *Oryza* (Ishimaru et al. 2001; Rae et al. 2006), suggesting that developmental integration may contribute to low variation in stomatal ratio between species of this genus (Giuliani et al. 2013). A second major limitation is that covariation in traits like stomatal length, which appear to be developmentally integrated on each surface, could be caused by other processes. For example, since stomatal size affects the speed and mechanics of stomatal closure (Drake et al. 2013; Harrison et al. 2020; but see Roddy et al. 2020), there may be strong selection for similar stomatal size throughout the leaf to harmonize rates of stomatal closure. Coordination between epidermal and mesophyll development may also constrain how independently stomatal traits on each surface can evolve (Dow et al. 2017; Lundgren et al. 2019; Thérroux-Rancourt et al. 2021; Borsuk et al. 2022).

Future research should identify the mechanistic basis of developmental disintegration between  $D_{ab}$  and  $D_{ad}$ . Multiple reviews of stomatal development conclude that stomatal traits are independently controlled on each surface (Lake et al. 2002; Bergmann and Sack 2007), but we do not know much about linkage between ab-adaxial polarity and stomatal development (Kidner and Timmermans 2010; Pillitteri and Torii 2012). Systems that have natural variation in stomatal ratio should allow us to study how developmental disintegration evolves. Quantitative genetic studies in *Brassica oleracea* L., *Oryza sativa* L., *Populus trichocarpa* Torr. & A. Gray ex Hook., *Populus* interspecific crosses, and *Solanum* interspecific crosses typically find partial independence of  $D_{ab}$  and  $D_{ad}$ : some loci affect both traits, but some loci only affect density on one surface and/or genetic correlations are weak (Ishimaru et al. 2001; Ferris et al. 2002; Hall et al. 2005; Rae et al. 2006; Laza et al. 2010; Chitwood et al. 2013; McKown et al. 2014; Muir et al. 2014; Porth et al. 2015; Fetter et al. 2021). For example, *Populus trichocarpa* populations have putatively adaptive genetic variation in  $D_{ad}$ . Populations are more amphistomatous at northern latitudes with shorter growing seasons that may select for faster carbon assimilation (McKown et al. 2014; Kaluthota et al. 2015; Porth et al. 2015). Genetic variation in key stomatal development transcription factors is associated with latitudinal variation in  $D_{ab}$ , which should help reveal the mechanistic basis of developmental disintegration between surfaces (McKown et al. 2019).

### Acknowledgments

E. J. Edwards proposed the idea of how developmental integration could explain bimodal stomatal ratio. Students

in the BIOL 470: Evolutionary Biology course at the University of Hawaii helped enter data from the literature. We thank Matt Pennell and Jacob Watts for comments on the manuscript. Jen Lau, Risa Sargent, Adam Roddy, and an anonymous reviewer provided helpful comments on the manuscript. C.D.M. was supported by an Evo-Devo-Eco Network (EDEN) research exchange (NSF IOS 0955517). The research was supported by project AGL2013-42364-R (Plan Nacional, Spain) and Universitat de les Illes Balears (UIB) grant 15/2105 awarded to J.G. We acknowledge Miquel Truyols and collaborators of the UIB Experimental Field and Greenhouses for their technical support. This is publication 178 from the School of Life Sciences, University of Hawaii at Mānoa.

### Statement of Authorship

C.D.M. led conceptualization, data analysis, and writing of the original draft. All authors collected data and assisted with review and editing.

### Data and Code Availability

The final data set and phylogeny used in the analysis are included in the supplemental PDF. The raw anatomical data and source code have been deposited in the Dryad Digital Repository (<https://doi.org/10.5061/dryad.0rxwdb42>; Muir et al. 2022).

### Literature Cited

- Anderson, S. A. S., and J. T. Weir. 2021. Diverge: evolutionary trait divergence between sister species and other paired lineages. <https://CRAN.R-project.org/package=diverge>.
- Armbruster, W. S. 1988. Multilevel comparative analysis of the morphology, function, and evolution of *Dalechampia* blossoms. *Ecology* 69:1746–1761. <https://doi.org/10.2307/1941153>.
- Armbruster, W. S., V. S. Di Stilio, J. D. Tuxill, T. C. Flores, and J. L. Velásquez Runk. 1999. Covariance and decoupling of floral and vegetative traits in nine Neotropical plants: a re-evaluation of Berg's correlation-pleiades concept. *American Journal of Botany* 86:39–55. <https://doi.org/10.2307/2656953>.
- Armbruster, W. S., C. Pélabon, G. H. Bolstad, and T. F. Hansen. 2014. Integrated phenotypes: understanding trait covariation in plants and animals. *Philosophical Transactions of the Royal Society B* 369:20130245. <https://doi.org/10.1098/rstb.2013.0245>.
- Arnold, S. J. 1992. Constraints on phenotypic evolution. *American Naturalist* 140:S85–S107.
- Barrett, S. C. H., and J. Hough. 2013. Sexual dimorphism in flowering plants. *Journal of Experimental Botany* 64:67–82. <https://doi.org/10.1093/jxb/ers308>.
- Beaulieu, J. M., I. J. Leitch, S. Patel, A. Pendharkar, and C. A. Knight. 2008. Genome size is a strong predictor of cell size and stomatal density in angiosperms. *New Phytologist* 179:975–986. <https://doi.org/10.1111/j.1469-8137.2008.02528.x>.

- Berg, R. L. 1959. A general evolutionary principle underlying the origin of developmental homeostasis. *American Naturalist* 93:103–105. <https://doi.org/10.1086/282061>.
- . 1960. The ecological significance of correlation pleiades. *Evolution* 14:171–180. <https://doi.org/10.2307/2405824>.
- Bergmann, D. C., and F. D. Sack. 2007. Stomatal development. *Annual Review of Plant Biology* 58:163–181. <https://doi.org/10.1146/annurev.arplant.58.032806.104023>.
- Berry, J. A., D. J. Beerling, and P. J. Franks. 2010. Stomata: key players in the earth system, past and present. *Current Opinion in Plant Biology* 13:232–239. <https://doi.org/10.1016/j.cpb.2010.04.013>.
- Borsuk, A. M., A. B. Roddy, G. Théroux-Rancourt, and C. R. Brodersen. 2022. Structural organization of the spongy mesophyll. *New Phytologist* 234:946–960. <https://doi.org/10.1111/nph.17971>.
- Brodribb, T. J., G. J. Jordan, and R. J. Carpenter. 2013. Unified changes in cell size permit coordinated leaf evolution. *New Phytologist* 199:559–570. <https://doi.org/10.1111/nph.12300>.
- Bucher, S. F., K. Auerswald, C. Grün-Wenzel, S. I. Higgins, J. G. Jorge, and C. Römermann. 2017. Stomatal traits relate to habitat preferences of herbaceous species in a temperate climate. *Flora* 229:107–115. <https://doi.org/10.1016/j.flora.2017.02.011>.
- Buckley, T. N., G. P. John, C. Scoffoni, and L. Sack. 2015. How does leaf anatomy influence water transport outside the xylem? *Plant Physiology* 168:1616–1635.
- Bürkner, P.-C. 2017. brms: an R package for Bayesian multilevel models using Stan. *Journal of Statistical Software* 80:1–28. <https://doi.org/10.18637/jss.v080.i01>.
- . 2018. Advanced Bayesian multilevel modeling with the R package brms. *R Journal* 10:395–411. <https://doi.org/10.32614/RJ-2018-017>.
- Casson, S., and J. E. Gray. 2008. Influence of environmental factors on stomatal development. *New Phytologist* 178:9–23. <https://doi.org/10.1111/j.1469-8137.2007.02351.x>.
- Chitwood, D. H., R. Kumar, L. R. Headland, A. Ranjan, M. F. Covington, Y. Ichihashi, D. Fulop, et al. 2013. A quantitative genetic basis for leaf morphology in a set of precisely defined tomato introgression lines. *Plant Cell* 25:2465–2481.
- Chitwood, D. H., D. T. Naylor, P. Thammapichai, A. C. S. Weeger, L. R. Headland, and N. R. Sinha. 2012. Conflict between intrinsic leaf asymmetry and phyllotaxis in the resupinate leaves of *Alstroemeria psittacina*. *Frontiers in Plant Science* 3:182. <https://doi.org/10.3389/fpls.2012.00182>.
- Clark, J. W., B. J. Harris, A. J. Hetherington, N. Hurtado-Castano, R. A. Brench, S. Casson, T. A. Williams, J. E. Gray, and A. M. Hetherington. 2022. The origin and evolution of stomata. *Current Biology* 32:R539–R553. <https://doi.org/10.1016/j.cub.2022.04.040>.
- Conner, J. K., and R. Lande. 2014. Raissa L. Berg's contributions to the study of phenotypic integration, with a professional biographical sketch. *Philosophical Transactions of the Royal Society B* 369:20130250. <https://doi.org/10.1098/rstb.2013.0250>.
- Deans, R. M., T. J. Brodribb, F. A. Busch, and G. D. Farquhar. 2020. Optimization can provide the fundamental link between leaf photosynthesis, gas exchange and water relations. *Nature Plants* 6:1116–1125. <https://doi.org/10.1038/s41477-020-00760-6>.
- de Boer, H. J., C. A. Price, F. Wagner-Cremer, S. C. Dekker, P. J. Franks, and E. J. Veneklaas. 2016. Optimal allocation of leaf epidermal area for gas exchange. *New Phytologist* 210:1219–1228. <https://doi.org/10.1111/nph.13929>.
- Dow, G. J., and D. C. Bergmann. 2014. Patterning and processes: how stomatal development defines physiological potential. *Current Opinion in Plant Biology* 21:67–74. <https://doi.org/10.1016/j.cpb.2014.06.007>.
- Dow, G. J., J. A. Berry, and D. C. Bergmann. 2014. The physiological importance of developmental mechanisms that enforce proper stomatal spacing in *Arabidopsis thaliana*. *New Phytologist* 201:1205–1217. <https://doi.org/10.1111/nph.12586>.
- . 2017. Disruption of stomatal lineage signaling or transcriptional regulators has differential effects on mesophyll development, but maintains coordination of gas exchange. *New Phytologist* 216:69–75. <https://doi.org/10.1111/nph.14746>.
- Drake, P. L., H. J. de Boer, S. J. Schymanski, and E. J. Veneklaas. 2019. Two sides to every leaf: water and CO<sub>2</sub> transport in hypostomatous and amphistomatous leaves. *New Phytologist* 222:1179–1187. <https://doi.org/10.1111/nph.15652>.
- Drake, P. L., R. H. Froend, and P. J. Franks. 2013. Smaller, faster stomata: scaling of stomatal size, rate of response, and stomatal conductance. *Journal of Experimental Botany* 64:495–505. <https://doi.org/10.1093/jxb/ers347>.
- Felsenstein, J. 1985. Phylogenies and the comparative method. *American Naturalist* 125:1–15.
- Ferris, R., L. Long, S. M. Bunn, K. M. Robinson, H. D. Bradshaw, A. M. Rae, and G. Taylor. 2002. Leaf stomatal and epidermal cell development: identification of putative quantitative trait loci in relation to elevated carbon dioxide concentration in poplar. *Tree Physiology* 22:633–640. <https://doi.org/10.1093/treephys/22.9.633>.
- Fetter, K. C., D. M. Nelson, and S. R. Keller. 2021. Growth-defense trade-offs masked in unadmixed populations are revealed by hybridization. *Evolution* 75:1450–1465. <https://doi.org/10.1111/evo.14227>.
- Franks, P. J., and D. J. Beerling. 2009. Maximum leaf conductance driven by CO<sub>2</sub> effects on stomatal size and density over geologic time. *Proceedings of the National Academy of Sciences of the USA* 106:10343–10347.
- Franks, P. J., and G. D. Farquhar. 2001. The effect of exogenous abscisic acid on stomatal development, stomatal mechanics, and leaf gas exchange in *Tradescantia virginiana*. *Plant Physiology* 125:935–942. <https://doi.org/10.1104/pp.125.2.935>.
- Gabry, J., and R. Češnovar. 2022. CmdStanR: R interface to CmdStan. <https://mc-stan.org/cmdstanr>, <https://discourse.mc-stan.org>.
- Galmés, J., J. M. Ochogavía, J. Gago, E. J. Roldán, J. Cifre, and M. À. Conesa. 2013. Leaf responses to drought stress in Mediterranean accessions of *Solanum lycopersicum*: anatomical adaptations in relation to gas exchange parameters. *Plant, Cell and Environment* 36:920–935. <https://doi.org/10.1111/pce.12022>.
- Gibson, A. C. 1996. *Structure-function relations of warm desert plants*. Springer, Berlin.
- Giuliani, R., N. Koteyeva, E. Voznesenskaya, M. A. Evans, A. B. Cousins, and G. E. Edwards. 2013. Coordination of leaf photosynthesis, transpiration, and structural traits in rice and wild relatives (genus *Oryza*). *Plant Physiology* 162:1632–1651.
- Gutschick, V. P. 1984. Photosynthesis model for C<sub>3</sub> leaves incorporating CO<sub>2</sub> transport, propagation of radiation, and biochemistry 1. Kinetics and their parameterization. *Photosynthetica* 18:549–568.
- Hall, N. M., H. Griffiths, J. A. Corlett, H. G. Jones, J. Lynn, and G. J. King. 2005. Relationships between water-use traits and photosynthesis in *Brassica oleracea* resolved by quantitative genetic analysis. *Plant Breeding* 124:557–564. <https://doi.org/10.1111/j.1439-0523.2005.01164.x>.
- Hansen, T. F. 2003. Is modularity necessary for evolvability? *Biosystems* 69:83–94. [https://doi.org/10.1016/S0303-2647\(02\)00132-6](https://doi.org/10.1016/S0303-2647(02)00132-6).

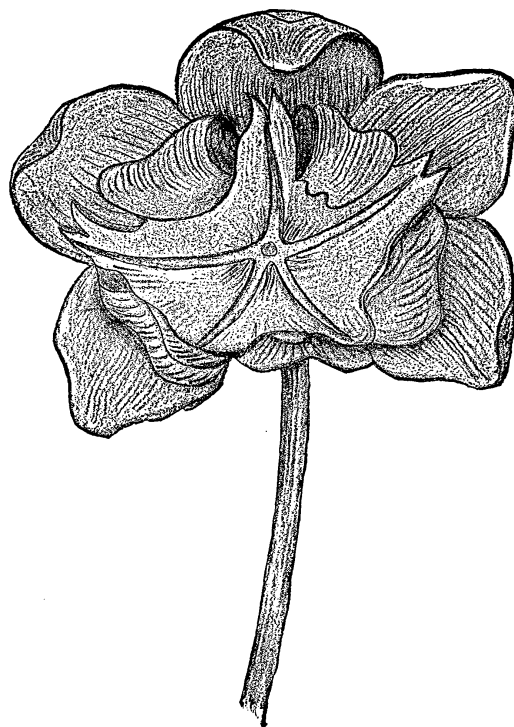
- Harrison, E. L., L. A. Cubas, J. E. Gray, and C. Hepworth. 2020. The influence of stomatal morphology and distribution on photosynthetic gas exchange. *Plant Journal* 101:768–779. <https://doi.org/10.1111/tpj.14560>.
- Haworth, M., C. Elliott-Kingston, and J. C. McElwain. 2013. Coordination of physiological and morphological responses of stomata to elevated [CO<sub>2</sub>] in vascular plants. *Oecologia* 171:71–82. <https://doi.org/10.1007/s00442-012-2406-9>.
- Henry, C., G. P. John, R. Pan, M. K. Bartlett, L. R. Fletcher, C. Scoffoni, and L. Sack. 2019. A stomatal safety-efficiency trade-off constrains responses to leaf dehydration. *Nature Communications* 10:3398. <https://doi.org/10.1038/s41467-019-11006-1>.
- Hetherington, A. M., and F. I. Woodward. 2003. The role of stomata in sensing and driving environmental change. *Nature* 424:901–908. <https://doi.org/10.1038/nature01843>.
- Ishimaru, K., K. Shirota, M. Higa, and Y. Kawamitsu. 2001. Identification of quantitative trait loci for adaxial and abaxial stomatal frequencies in *Oryza sativa*. *Plant Physiology and Biochemistry* 39:173–177. [https://doi.org/10.1016/S0981-9428\(00\)01232-8](https://doi.org/10.1016/S0981-9428(00)01232-8).
- Jordan, G. J., R. J. Carpenter, and T. J. Brodribb. 2014. Using fossil leaves as evidence for open vegetation. *Palaeogeography, Palaeoclimatology, Palaeoecology* 395:168–175. <https://doi.org/10.1016/j.palaeo.2013.12.035>.
- Jordan, G. J., R. J. Carpenter, A. Koutoulis, A. Price, and T. J. Brodribb. 2015. Environmental adaptation in stomatal size independent of the effects of genome size. *New Phytologist* 205:608–617. <https://doi.org/10.1111/nph.13076>.
- Kaluthota, S., D. W. Pearce, L. M. Evans, M. G. Letts, T. G. Whitham, and S. B. Rood. 2015. Higher photosynthetic capacity from higher latitude: foliar characteristics and gas exchange of southern, central and northern populations of *Populus angustifolia*. *Tree Physiology* 35:936–948. <https://doi.org/10.1093/treephys/tpv069>.
- Kelly, C. K., and D. J. Beerling. 1995. Plant life form, stomatal density and taxonomic relatedness: a reanalysis of Salisbury (1927). *Functional Ecology* 9:422–431. <https://doi.org/10.2307/2390005>.
- Kidner, C. A., and M. C. P. Timmermans. 2010. Signaling sides. *Current Topics in Developmental Biology* 91:141–168. [https://doi.org/10.1016/S0070-2153\(10\)91005-3](https://doi.org/10.1016/S0070-2153(10)91005-3).
- Lake, J. A., F. I. Woodward, and W. P. Quick. 2002. Long-distance CO<sub>2</sub> signalling in plants. *Journal of Experimental Botany* 53:183–193. <https://doi.org/10.1093/jexbot/53.367.183>.
- Lande, R. 1979. Quantitative genetic analysis of multivariate evolution, applied to brain:body size allometry. *Evolution* 33:402–416. <https://doi.org/10.2307/2407630>.
- Lange, K. L., R. J. A. Little, and J. M. G. Taylor. 1989. Robust statistical modeling using the *t* distribution. *Journal of the American Statistical Association* 84:881–896. <https://doi.org/10.1080/01621459.1989.10478852>.
- Lawson, T., and J. Matthews. 2020. Guard cell metabolism and stomatal function. *Annual Review of Plant Biology* 71:273–302. <https://doi.org/10.1146/annurev-arplant-050718-100251>.
- Laza, M. R. C., M. Kondo, O. Ideta, E. Barlaan, and T. Imbe. 2010. Quantitative trait loci for stomatal density and size in lowland rice. *Euphytica* 172:149–158. <https://doi.org/10.1007/s10681-009-0011-8>.
- Lehmann, P., and D. Or. 2015. Effects of stomata clustering on leaf gas exchange. *New Phytologist* 207:1015–1025. <https://doi.org/10.1111/nph.13442>.
- Leitch, I. J., E. Johnston, J. Pellicer, O. Hidalgo, and M. D. Bennett. 2019. Angiosperm DNA C-values database. <https://cvalues.science.kew.org/>.
- Liu, C., N. He, J. Zhang, Y. Li, Q. Wang, L. Sack, and G. Yu. 2018. Variation of stomatal traits from cold temperate to tropical forests and association with water use efficiency. *Functional Ecology* 32:20–28. <https://doi.org/10.1111/1365-2435.12973>.
- Liu, C., C. D. Muir, Y. Li, L. Xu, M. Li, J. Zhang, H. J. de Boer, et al. 2021. Scaling between stomatal size and density in forest plants.” *bioRxiv*, <https://doi.org/10.1101/2021.04.25.441252>.
- Lundgren, M. R., A. Mathers, A. L. Baillie, J. Dunn, M. J. Wilson, L. Hunt, R. Pajor, et al. 2019. Mesophyll porosity is modulated by the presence of functional stomata. *Nature Communications* 10:2825. <https://doi.org/10.1038/s41467-019-10826-5>.
- Lynch, M., and B. Walsh. 1998. *Genetics and analysis of quantitative traits*. Sinauer, Sunderland, MA.
- Mackenzie, D. 1999. Proving the perfection of the honeycomb. *Science* 285:1338–1339. <https://doi.org/10.1126/science.285.5432.1338>.
- Magallón, S., S. Gómez-Acevedo, L. L. Sánchez-Reyes, and T. Hernández-Hernández. 2015. A metacalibrated time-tree documents the early rise of flowering plant phylogenetic diversity. *New Phytologist* 207:437–453. <https://doi.org/10.1111/nph.13264>.
- Maritan, A., C. Micheletti, A. Trovato, and J. R. Banavar. 2000. Optimal shapes of compact strings. *Nature* 406:287–290. <https://doi.org/10.1038/35018538>.
- Maynard Smith, J., R. Burian, S. Kauffman, P. Alberch, J. Campbell, B. Goodwin, R. Lande, D. Raup, and L. Wolpert. 1985. Developmental constraints and evolution: a perspective from the Mountain Lake Conference on Development and Evolution. *Quarterly Review of Biology* 60:265–287. <https://www.jstor.org/stable/2828504>.
- McGhee, G. R. 1999. *Theoretical morphology: the concept and its applications*. Perspectives in Paleobiology and Earth History. Columbia University Press, New York.
- . 2007. *The geometry of evolution: adaptive landscapes and theoretical morphospaces*. Cambridge University Press, Cambridge.
- McKown, A. D., R. D. Guy, L. Quamme, J. Klápště, J. La Mantia, C. P. Constabel, Y. A. El-Kassaby, R. C. Hamelin, M. Zifkin, and M. S. Azam. 2014. Association genetics, geography and eco-physiology link stomatal patterning in *Populus trichocarpa* with carbon gain and disease resistance trade-offs. *Molecular Ecology* 23:5771–5790. <https://doi.org/10.1111/mec.12969>.
- McKown, A. D., J. Klápště, R. D. Guy, O. R. A. Corea, S. Fritsche, J. Ehrling, Y. A. El-Kassaby, and S. D. Mansfield. 2019. A role for *SPEECHLESS* in the integration of leaf stomatal patterning with the growth vs disease trade-off in poplar. *New Phytologist* 223:1888–1903. <https://doi.org/10.1111/nph.15911>.
- Metcalfe, C. R., and L. Chalk. 1950. *Anatomy of the dicotyledons*. Vols. 1, 2. Oxford University Press, Oxford.
- Mitchison, G. J. 1977. Phyllotaxis and the Fibonacci series: an explanation is offered for the characteristic spiral leaf arrangement found in many plants. *Science* 196:270–275. <https://doi.org/10.1126/science.196.4287.270>.
- Mott, K. A., A. C. Gibson, and J. W. O’Leary. 1982. The adaptive significance of amphistomatic leaves. *Plant, Cell and Environment* 5:455–460. <https://doi.org/10.1111/1365-3040.ep11611750>.
- Muir, C. D. 2015. Making pore choices: repeated regime shifts in stomatal ratio. *Proceedings of the Royal Society B* 282:20151498. <https://doi.org/10.1098/rspb.2015.1498>.
- . 2018. Light and growth form interact to shape stomatal ratio among British angiosperms. *New Phytologist* 218:242–252.
- . 2019. Is amphistomy an adaptation to high light? optimality models of stomatal traits along light gradients. *Integrative and Comparative Biology* 59:571–584. <https://doi.org/10.1093/icb/icz085>.

- Muir, C. D., M. À. Conesa, J. Galmés, V. S. Pathare, P. Rivera, R. López Rodríguez, T. Terrazas, and D. Xiong. 2022. Data from: How important are functional and developmental constraints on phenotypic evolution? an empirical test with the stomatal anatomy of flowering plants. *American Naturalist*, Dryad Digital Repository, <https://doi.org/10.5061/dryad.0rxwdb42>.
- Muir, C. D., J. B. Pease, and L. C. Moyle. 2014. Quantitative genetic analysis indicates natural selection on leaf phenotypes across wild tomato species (*Solanum* sect. *Lycopersicon*; Solanaceae). *Genetics* 198:1629–1643. <https://doi.org/10.1534/genetics.114.169276>.
- Murray, M., W. K. Soh, C. Yiotis, R. A. Spicer, T. Lawson, and J. C. McElwain. 2020. Consistent relationship between field-measured stomatal conductance and theoretical maximum stomatal conductance in C<sub>3</sub> woody angiosperms in four major biomes. *International Journal of Plant Sciences* 181:142–154. <https://doi.org/10.1086/706260>.
- Niklas, K. J. 1988. The role of phyllotactic pattern as a “developmental constraint” on the interception of light by leaf surfaces. *Evolution* 42:1–16. <https://doi.org/10.2307/2409111>.
- Olson, M. E. 2019. Plant evolutionary ecology in the age of the extended evolutionary synthesis. *Integrative and Comparative Biology* 59:493–502. <https://doi.org/10.1093/icb/icz042>.
- Olson, M. E., and A. Arroyo-Santos. 2015. How to study adaptation (and why to do it that way). *Quarterly Review of Biology* 90:167–191. <https://doi.org/10.1086/681438>.
- Parkhurst, D. F. 1978. The adaptive significance of stomatal occurrence on one or both surfaces of leaves. *Journal of Ecology* 66:367–383. <https://doi.org/10.2307/2259142>.
- Parkhurst, D. F., and K. A. Mott. 1990. Intercellular diffusion limits to CO<sub>2</sub> uptake in leaves: studies in air and helox. *Plant Physiology* 94:1024–1032. <https://doi.org/10.1104/pp.94.3.1024>.
- Pathare, V. S., N. Koteyeva, and A. B. Cousins. 2020. Increased adaxial stomatal density is associated with greater mesophyll surface area exposed to intercellular air spaces and mesophyll conductance in diverse C<sub>4</sub> grasses. *New Phytologist* 225:169–182. <https://doi.org/10.1111/nph.16106>.
- Peat, H. J., and A. H. Fitter. 1994. A comparative study of the distribution and density of stomata in the British flora. *Biological Journal of the Linnean Society* 52:377–393.
- Pélabon, C., C. Firmat, G. H. Bolstad, K. L. Voje, D. Houle, J. Casarsa, A. Le Rouzic, and T. F. Hansen. 2014. Evolution of morphological allometry: the evolvability of allometry. *Annals of the New York Academy of Sciences* 1320:58–75. <https://doi.org/10.1111/nyas.12470>.
- Pellicer, J., and I. J. Leitch. 2020. The plant DNA C-values database (release 7.1): an updated online repository of plant genome size data for comparative studies. *New Phytologist* 226:301–305. <https://doi.org/10.1111/nph.16261>.
- Pillitteri, L. J., and K. U. Torii. 2012. Mechanisms of stomatal development. *Annual Review of Plant Biology* 63:591–614. <https://doi.org/10.1146/annurev-arplant-042811-105451>.
- Porth, I., J. Klápště, A. D. McKown, J. La Mantia, R. D. Guy, P. K. Ingvarsson, R. Hamelin, et al. 2015. Evolutionary quantitative genomics of *Populus trichocarpa*. *PLoS ONE* 25:e0142864.
- R Core Team. 2022. R: a language and environment for statistical computing. R Foundation for Statistical Computing, Vienna. <http://www.R-project.org/>.
- Rae, A. M., R. Ferris, M. J. Tallis, and G. Taylor. 2006. Elucidating genomic regions determining enhanced leaf growth and delayed senescence in elevated CO<sub>2</sub>. *Plant, Cell and Environment* 29:1730–1741. <https://doi.org/10.1111/j.1365-3040.2006.01545.x>.
- Raup, D. M. 1966. Geometric analysis of shell coiling: general problems. *Journal of Paleontology* 40:1178–1190. <https://www.jstor.org/stable/1301992>.
- Reinhardt, D., and E. M. Gola. 2022. Law and order in plants—the origin and functional relevance of phyllotaxis. *Trends in Plant Science* 27:1017–1032. <https://doi.org/10.1016/j.tplants.2022.04.005>.
- Roddy, A. B., C. M. Williams, T. Lilitham, J. Farmer, V. Wormser, T. Pham, P. V. A. Fine, T. S. Feild, and T. E. Dawson. 2013. Uncorrelated evolution of leaf and petal venation patterns across the angiosperm phylogeny. *Journal of Experimental Botany* 64:4081–4088. <https://doi.org/10.1093/jxb/ert247>.
- Roddy, A. B., G. Thérout-Rancourt, T. Abbo, J. W. Benedetti, C. R. Brodersen, M. Castro, S. Castro, et al. 2020. The scaling of genome size and cell size limits maximum rates of photosynthesis with implications for ecological strategies. *International Journal of Plant Sciences* 181:75–87. <https://doi.org/10.1086/706186>.
- Royer, D. L. 2001. Stomatal density and stomatal index as indicators of paleoatmospheric CO<sub>2</sub> concentration. *Review of Palaeobotany and Palynology* 114:1–28. [https://doi.org/10.1016/S0034-6667\(00\)00074-9](https://doi.org/10.1016/S0034-6667(00)00074-9).
- Sack, L., and T. N. Buckley. 2016. The developmental basis of stomatal density and flux. *Plant Physiology* 171:2358–2363. <https://doi.org/10.1104/pp.16.00476>.
- Sack, L., P. D. Cowan, N. Jaikumar, and N. M. Holbrook. 2003. The “hydrology” of leaves: co-ordination of structure and function in temperate woody species. *Plant, Cell and Environment* 26:1343–1356. <https://doi.org/10.1046/j.0016-8025.2003.01058.x>.
- Salisbury, E. J. 1928. I. On the causes and ecological significance of stomatal frequency, with special reference to the woodland flora. *Philosophical Transactions of the Royal Society B* 216:1–65. <https://doi.org/10.1098/rstb.1928.0001>.
- Schluter, D. 1996. Adaptive radiation along genetic lines of least resistance. *Evolution* 50:1766–1774. <https://doi.org/10.2307/2410734>.
- Simonin, K. A., and A. B. Roddy. 2018. Genome downsizing, physiological novelty, and the global dominance of flowering plants. *PLoS Biology* 16:e2003706. <https://doi.org/10.1371/journal.pbio.2003706>.
- Šimová, I., and T. Herben. 2012. Geometrical constraints in the scaling relationships between genome size, cell size and cell cycle length in herbaceous plants. *Proceedings of the Royal Society B* 279:867–875. <https://doi.org/10.1098/rspb.2011.1284>.
- Smith, S. A., and J. W. Brown. 2018. Constructing a broadly inclusive seed plant phylogeny. *American Journal of Botany* 105:302–314. <https://doi.org/10.1002/ajb2.1019>.
- Smith, W. K., D. T. Bell, and K. A. Shepherd. 1998. Associations between leaf structure, orientation, and sunlight exposure in five Western Australian communities. *American Journal of Botany* 85:51–63.
- Stan Development Team. 2022. Stan modeling language users guide and reference manual. <https://mc-stan.org>.
- Thérout-Rancourt, G., A. B. Roddy, J. M. Earles, M. E. Gilbert, M. A. Zwieniecki, C. K. Boyce, D. Tholen, A. J. McElrone, K. A. Simonin, and C. R. Brodersen. 2021. Maximum CO<sub>2</sub> diffusion inside leaves is limited by the scaling of cell size and genome size. *Proceedings of the Royal Society B* 288:20203145. <https://doi.org/10.1098/rspb.2020.3145>.
- Vehtari, A., A. Gelman, D. Simpson, B. Carpenter, and P.-C. Bürkner. 2021. Rank-normalization, folding, and localization: an

- improved  $\hat{R}$  for assessing convergence of MCMC (with discussion). *Bayesian Analysis* 16:667–718. <https://doi.org/10.1214/20-BA1221>.
- Weiss, A. 1865. Untersuchungen Über Die Zahlen-Und Grössenverhältnisse Der Spaltöffnungen. *Jahrbücher Für Wissenschaftliche Botanik* 4:125–196.
- Woodward, F. I. 1987. Stomatal numbers are sensitive to increases in CO<sub>2</sub> from pre-industrial levels. *Nature* 327:617–618.
- Zanne, A. E., D. C. Tank, W. K. Cornwell, J. M. Eastman, S. A. Smith, R. G. FitzJohn, D. J. McGlenn, et al. 2014. Three keys to the radiation of angiosperms into freezing environments. *Nature* 506:89–92. <https://doi.org/10.1038/nature12872>.
- Zeiger, E., G. D. Farquhar, and I. R. Cowan, eds. 1987. *Stomatal function*. Stanford University Press, Stanford, CA.
- ### References Cited Only in the Online Enhancements
- Arambarri, A. M., S. A. Stenglein, M. N. Colares, and M. C. Novoa. 2005. Taxonomy of the New World species of lotus (Leguminosae: Loteae). *Australian Journal of Botany* 53:797–812. <https://doi.org/10.1071/BT04101>.
- Avita, S. R., and J. A. Inamdar. 1980. Structure and ontogeny of stomata in Ranunculaceae and Paeoniaceae. *Flora* 170:354–370. [https://doi.org/10.1016/S0367-2530\(17\)31224-0](https://doi.org/10.1016/S0367-2530(17)31224-0).
- Caldera, H. I. U., W. A. J. M. De Costa, F. I. Woodward, J. A. Lake, and S. M. W. Ranwala. 2017. Effects of elevated carbon dioxide on stomatal characteristics and carbon isotope ratio of *Arabidopsis thaliana* ecotypes originating from an altitudinal gradient. *Physiologia Plantarum* 159:74–92. <https://doi.org/10.1111/ppl.12486>.
- Chamberlain, S. A., and E. Szöcs. 2013. Taxize: taxonomic search and retrieval in R. *F1000Research* 2:191. <https://doi.org/10.12688/f1000research.2-191.v2>.
- Chandra, V. 1967. Epidermal studies on some solanaceous plants. *Indian Journal of Pharmacy* 29:227–229.
- Conesa, M. À., C. D. Muir, A. Molins, and J. Galmés. 2019. Stomatal anatomy coordinates leaf size with Rubisco kinetics in the Balaric *Limonium*. *AoB Plants* 12:plz050. <https://doi.org/10.1093/aobpla/plz050>.
- Dow, G. J., D. C. Bergmann, and J. A. Berry. 2014. An integrated model of stomatal development and leaf physiology. *New Phytologist* 201:1218–1226.
- Eckerson, S. H. 1908. The number and size of the stomata. *Botanical Gazette* 46:221–224.
- Gindel, I. 1969. Stomatal number and size as related to soil moisture in tree xerophytes in Israel. *Ecology* 50:263–267.
- Hanafy, D. M., P. D. Prenzler, R. A. Hill, and G. E. Burrows. 2019. Leaf micromorphology of 19 *Mentha* taxa. *Australian Journal of Botany* 67:463–472. <https://doi.org/10.1071/BT19054>.
- Huang, S. 2019. Leaf functional traits as predictors of drought tolerance in urban trees. Master's thesis. California Polytechnic State University, San Luis Obispo.
- Jin, Y., and H. Qian. 2019. V.PhyloMaker: an R package that can generate very large phylogenies for vascular plants. *Ecography* 42:1353–1359. <https://doi.org/10.1111/ecog.04434>.
- Juhász, M. 1966. Effect of ecological factors on the leaf epidermis of species *Solanum*. *Acta Biologica* 12:29–36.
- . 1968. A comparative histological examination of the leaf epidermis of some *Solanum* species. *Acta Biologica* 14:5–9.
- Kannabiran, B., and V. Ramassamy. 1988. Foliar epidermis and taxonomy in Apocynaceae. *Proceedings of the Indian Academy of Sciences* 98:409–417.
- Kawamitsu, Y., S. Hiyane, S. Murayama, A. Nose, and C. Shinjyo. 1996. Stomatal frequency and guard cell length in C<sub>3</sub> and C<sub>4</sub> grass species. *Japanese Journal of Crop Science* 65:626–633.
- Khan, R., S. Z. U. Abidin, M. Ahmad, M. Zafar, J. Liu, Lubna, S. Jamshed, and Ö. Kiliç. 2019. Taxonomic importance of SEM and LM foliar epidermal micro-morphology: a tool for robust identification of gymnosperms. *Flora* 255:42–68. <https://doi.org/10.1016/j.flora.2019.03.016>.
- Kim, I. 1987. Comparative anatomy of some parents and hybrids of the Hawaiian Madiinae (Asteraceae). *American Journal of Botany* 74:1224–1238. <https://doi.org/10.2307/2444158>.
- McKown, A. D., M. E. Akamine, and L. Sack. 2016. Trait convergence and diversification arising from a complex evolutionary history in Hawaiian of *Scaevola*. *Oecologia* 181:1083–1100. <https://doi.org/10.1007/s00442-016-3640-3>.
- Missouri Botanical Garden. 2020. Tropicos. <https://tropicos.org>.
- Ouellette, B. F. F., and M. S. Boguski. 1997. Database divisions and homology search files: a guide for the perplexed. *Genome Research* 7:952–955. <https://doi.org/10.1101/gr.7.10.952>.
- Pallardy, S. G., and T. T. Kozlowski. 1979. Frequency and length of stomata of 21 *Populus* clones. *Canadian Journal of Botany* 57:2519–2523.
- Pandey, S., and P. K. Nagar. 2003. Patterns of leaf surface wetness in some important medicinal and aromatic plants of western Himalaya. *Flora* 198:349–357.
- Paradis, E., and K. Schliep. 2019. Ape 5.0: an environment for modern phylogenetics and evolutionary analyses in R. *Bioinformatics* 35:526–528. <https://doi.org/10.1093/bioinformatics/bty633>.
- Pennell, M. W., R. G. FitzJohn, and W. K. Cornwell. 2016. A simple approach for maximizing the overlap of phylogenetic and comparative data. *Methods in Ecology and Evolution* 7:751–758.
- Price, H. J., A. H. Sparrow, and A. F. Nauman. 1973. Correlations between nuclear volume, cell volume and DNA content in meristematic cells of herbaceous angiosperms. *Experientia* 29:1028–1029. <https://doi.org/10.1007/BF01930444>.
- Rees, J., and K. Cranston. 2017. Automated assembly of a reference taxonomy for phylogenetic data synthesis. *Biodiversity Data Journal* 5:e12581. <https://doi.org/10.3897/BDJ.5.e12581>.
- Rivera, P., J. L. Villaseñor, and T. Terrazas. 2017. Meso- or xeromorphic? foliar characters of Asteraceae in a xeric scrub of Mexico. *Botanical Studies* 58:12. <https://doi.org/10.1186/s40529-017-0166-x>.
- Royal Botanic Gardens, Kew, Harvard University Herbaria and Libraries, and Australian National Botanic Gardens. 2020. International plant names index. <http://www.ipni.org>.
- Scalon, M. C., D. R. Rossatto, F. M. C. B. Domingos, and A. C. Franco. 2016. Leaf morphophysiology of a Neotropical mistletoe is shaped by seasonal patterns of host leaf phenology. *Oecologia* 180:1103–1112. <https://doi.org/10.1007/s00442-015-3519-8>.
- Siddiqi, M. R., S. Ahmad, and Z.-U. Rehman. 1991. A contribution to the study of epidermis in some members of the family Euphorbiaceae. Pages 169–82 in S. I. Ali and A. Ghaffar, eds. *Plant life of South Asia*. Department of Botany, University of Karachi, Pakistan.
- Smith, S. A., and J. F. Walker. 2019. PyPHLAWD: a Python tool for phylogenetic dataset construction. *Methods in Ecology and Evolution* 10:104–108. <https://doi.org/10.1111/2041-210X.13096>.
- Sporck, M. J. 2011. The Hawaiian C<sub>4</sub> *Euphorbia* adaptive radiation: an ecophysiological approach to understanding leaf trait variation. PhD diss. University of Hawaii.

- Stamatakis, A. 2014. RAxML version 8: a tool for phylogenetic analysis and post-analysis of large phylogenies. *Bioinformatics* 30:1312–1313.
- Stenglein, S. A., A. M. Arambarri, M. N. Colares, M. C. Novoa, and C. E. Vizcaino. 2003a. Leaf epidermal characteristics of *Lotus* subgenus *Acmispon* (Fabaceae: Loteae) and a numerical taxonomic evaluation. *Canadian Journal of Botany* 81:933–944. <https://doi.org/10.1139/b03-090>.
- . 2003b. Leaf epidermal characteristics of *Lotus* subgenus *Acmispon* (Fabaceae: Loteae) and a numerical taxonomic evaluation. *Canadian Journal of Botany* 81:933–944. <https://doi.org/10.1139/b03-090>.
- Sundberg, M. D. 1986. A comparison of stomatal distribution and length in succulent and non-succulent desert plants. *Phytomorphology* 36:53–66.
- Szymura, M., and K. Wolski. 2011. Leaf epidermis traits as tools to identify *Solidago* L. taxa in Poland. *Acta Biologica Cracoviensia Series Botanica* 53:38–46. <https://doi.org/10.2478/v10182-011-0006-3>.
- US Department of Agriculture, Agricultural Research Service. 2020. Germplasm resources information network. <http://www.ars-grin.gov/>.
- Wagner, G. P. 1989. Multivariate mutation-selection balance with constrained pleiotropic effects. *Genetics* 122:223–234. <https://doi.org/10.1093/genetics/122.1.223>.
- Xiong, D., and J. Flexas. 2020. From one side to two sides: the effects of stomatal distribution on photosynthesis. *New Phytologist* 228:1754–1766. <https://doi.org/10.1111/nph.16801>.
- Yang, X., Y. Yang, C. Ji, T. Feng, Y. Shi, L. Lin, J. Ma, and J.-S. He. 2014. Large-scale patterns of stomatal traits in Tibetan and Mongolian grassland species. *Basic and Applied Ecology* 15:122–132. <https://doi.org/10.1016/j.baae.2014.01.003>.
- Zarinkamar, F. 2006. Density, size and distribution of stomata in different monocotyledons. *Pakistan Journal of Biological Sciences* 9:1650–1659.
- . 2007. Stomatal observations in dicotyledons. *Pakistan Journal of Biological Sciences* 10:199–219.
- Zhao, W., P. Fu, G. Liu, and P. Zhao. 2020. Difference between emergent aquatic and terrestrial monocotyledonous herbs in relation to the coordination of leaf stomata with vein traits. *AoB Plants* 12:plaa047. <https://doi.org/10.1093/aobpla/plaa047>.
- Zlatković, B., Z. S. Mitić, S. Jovanović, D. Lakušić, B. Lakušić, J. Rajković, and G. Stojanović. 2017. Epidermal structures and composition of epicuticular waxes of *Sedum album sensu lato* (Crasulaceae) in Balkan Peninsula. *Plant Biosystems* 151:974–984. <https://doi.org/10.1080/11263504.2016.1218971>.
- Zoric, L., L. Merkulov, J. Lukovic, P. Boza, and D. Polic. 2009. Leaf epidermal characteristics of *Trifolium* L. species from Serbia and Montenegro. *Flora* 204:198–209. <https://doi.org/10.1016/j.flora.2008.02.002>.

Associate Editor: Risa D. Sargent  
Editor: Jennifer A. Lau



“Sarracenia.” From “How the Pitcher Plant Got Its Leaves” by Joseph F. James (*The American Naturalist*, 1885, 19:567–578).